Check for updates

A Gas-and-Brake Mechanism of bHLH Proteins Modulates Shade Avoidance[1][OPEN]

Sara Buti, Chrysoula K. Pantazopoulou, Kasper van Gelderen, Valérie Hoogers, Emilie Reinen,[2] and Ronald Pierik[3,4]

Plant Ecophysiology, Institute of Environmental Biology, Utrecht University, Kruytgebouw, 3584 CH Utrecht, the Netherlands

ORCID IDs: 0000-0003-4879-2265 (S.B.); 0000-0001-5412-6029 (C.K.P.); 0000-0001-7809-2812 (K.v.G.); 0000-0003-3533-8207 (V.H.); 0000-0001-7114-5336 (E.R.); 0000-0002-5320-6817 (R.P.)

Plants detect proximity of competitors through reduction in the ratio between red and far-red light that triggers the shade avoidance syndrome, inducing responses such as accelerated shoot elongation and early flowering. Shade avoidance is regulated by PHYTOCHROME INTERACTING FACTORs, a group of basic helix-loop-helix (bHLH) transcription factors. Another (b)HLH protein, KIDARI (KDR), which is non-DNA-binding, was identified in de-etiolation studies and proposed to interact with LONG HYPOCOTYL IN FAR-RED1 (HFR1), a (b)HLH protein that inhibits shade avoidance. Here, we established roles of KDR in regulating shade avoidance in Arabidopsis (*Arabidopsis thaliana*) and investigated how KDR regulates the shade avoidance network. We showed that KDR is a positive regulator of shade avoidance and interacts with several negative growth regulators. We identified KDR interactors using a combination of yeast two-hybrid screening and dedicated confirmations with bimolecular fluorescence complementation. We demonstrated that KDR is translocated primarily to the nucleus when coexpressed with these interactors. A genetic approach confirmed that several of these interactions play a functional role in shade avoidance; however, we propose that KDR does not interact with HFR1 to regulate shade avoidance. Based on these observations, we propose that shade avoidance is regulated by a three-layered gas-and-brake mechanism of bHLH protein interactions, adding a layer of complexity to what was previously known.

Plants harvest light energy during photosynthesis, especially blue (B; ~400–500 nm wavelengths) and red (R; ~600–700 nm wavelengths) light, while mostly reflecting far-red light (FR; ~700–800 nm wavelengths). As a consequence, the ratio of R to FR is reduced by light reflected or transmitted through plant leaves and neighbors use this to detect the presence of nearby plants. Shade intolerant plants, such as Arabidopsis (*Arabidopsis thaliana*), respond to this lowered R:FR ratio with the shade avoidance syndrome (SAS). The main shade avoidance characteristics in Arabidopsis are hypocotyl, internode, and petiole elongation; early flowering; and upward leaf movement called hyponasty (Ballaré et al., 1991; de Wit et al., 2015, 2016; Pantazopoulou et al., 2017; Galvão et al., 2019). SAS is typical of most plants, including crops, and although it improves individual plant fitness, it may compromise total crop yield (Robson et al., 1996; Boccalandro et al., 2003). By contrast, shade-tolerant species, such as those from forest understories, have developed alternative strategies to cope with shade conditions without investing in shade avoidance growth (Gommers et al., 2013, 2017; Molina-Contreras et al., 2019).

In an attempt to unravel the strategy of SAS suppression in some species, Gommers et al. (2017) previously described the contrasting shade-tolerant and -intolerant responses of two selected *Geranium* species when exposed to low R:FR. In a transcriptome approach between these species, putative regulators of these two different responses were identified. One of these regulators is a basic helix-loop-helix (bHLH) protein-encoding gene, called *KIDARI (KDR)/PACLOBUTRAZOL RESISTANCE6* (*PRE6*; Gommers et al., 2017). The expression of *KDR* in Arabidopsis has been shown to rely on functional PHYTOCHROME-INTERACTING FACTOR4 (PIF4), PIF5, and PIF7 in both white light and low R:FR conditions (Gommers et al., 2017); however, the precise role of KDR in shade avoidance responses is poorly understood.

The main mechanism by which KDR has been previously shown to regulate growth in dark versus

[1]This work was supported by the Netherlands Organisation for Scientific Research (grant nos. VIDI 864.12.003, BBoL 737.016.012, VICI 865.17.002, to R.P.).

[2]Present address: Gadeta B.V., Yalelaan 62, 3584 CM Utrecht, the Netherlands.

[3]Author for contact: r.pierik@uu.nl.

[4]Senior author.

The author responsible for distribution of materials integral to the findings presented in this article in accordance with the policy described in the Instructions for Authors (www.plantphysiol.org) is: Ronald Pierik (r.pierik@uu.nl).

S.B. and R.P. designed the research; S.B., C.K.P., V.H., K.v.G., and E.R. performed the experiments; S.B. and R.P. wrote the article.

[OPEN]Articles can be viewed without a subscription.

www.plantphysiol.org/cgi/doi/10.1104/pp.20.00677

Downloaded on January 21, 2021. - Published by https://plantphysiol.org
Copyright (c) 2020 American Society of Plant Biologists. All rights reserved.

monochromatic light is by acting as a cofactor. KDR does not directly regulate gene transcription because it lacks the capability to bind DNA, but it is able to interfere with the action of other proteins. KDR cannot bind DNA directly because it misses specific amino acids (Glu and Arg) in the basic domain, which are essential for DNA binding (Hyun and Lee, 2006). Its function is mainly determined by the HLH domain, and through this domain, KDR was proposed to interact with LONG HYPOCOTYL IN FAR-RED1 (HFR1; Hyun and Lee, 2006; Hong et al., 2013), another non-DNA-binding (b)HLH protein. HFR1 is an established regulator of shade avoidance and binds to PIF proteins (Hornitschek et al., 2009), preventing them from activating the transcription of genes associated with SAS. HFR1 and PIF4 are both members of the bHLH transcription factor (TF) family, but whereas PIF4 promotes SAS through the transcriptional activation of specific genes, HFR1 plays a negative role in SAS by suppressing PIF4 action through direct binding (Sessa et al., 2005; Hornitschek et al., 2009). It is proposed that the regulation of both positive and negative regulators upon shade exposure helps plants tune the intensity of their shade avoidance responses (Sessa et al., 2005; de Wit et al., 2016; Gommers et al., 2017). *PIF4* and other members of the same subfamily, such as *PIF1*, *PIF3*, *PIF5*, and *PIF7*, are not transcriptionally upregulated in shade conditions, but their proteins are stabilized (Al-Sady et al., 2006; Shen et al., 2007; Leivar et al., 2008; Li et al., 2012; Lorrain and Fankhauser, 2012). In standard light, phytochromes are active and their interaction with PIFs leads to PIF inactivation and often degradation, whereas phytochromes are inactivated in shade, relieving the repression of PIF activity (Chen and Chory, 2011; Leivar and Quail, 2011). PIF proteins act as positive regulators of SAS primarily by promoting auxin synthesis, transport, and response (Hornitschek et al., 2012; Li et al., 2012). Simultaneously, PIFs also promote the expression of several negative regulators, such as *HFR1*, *PHYTOCHROME RAPIDLY REGULATED1* (*PAR1*), and *PAR2* (Sessa et al., 2005; Roig-Villanova et al., 2006), all non-DNA-binding (b)HLH proteins. Thus, there is a high redundancy as well as specification within the bHLH family in the regulation of SAS, allowing a highly flexible response that can integrate different environmental parameters.

In this study, we established the role of KDR in shade avoidance. Using established and novel Arabidopsis *kdr* mutant and overexpression lines, we demonstrated that KDR is a positive regulator of low R:FR-induced hypocotyl elongation. We showed that *KDR* overexpression, in addition to promoting hypocotyl elongation, also stimulates primary root elongation, bolting, and flowering. Using yeast two-hybrid (Y2H) and bimolecular fluorescence complementation (BiFC) approaches, we identified several interactors of KDR and showed that they colocalize with KDR in the nucleus. Experiments on mutants and transgenics to modulate the expression levels of these putative interactors, combined with published knowledge about these genes, suggest that all KDR-interacting proteins found here are themselves negative regulators of low R:FR-induced hypocotyl elongation. We propose that KDR interaction with these growth suppressors disables them from interacting with their downstream targets, alleviating the restraint on shade avoidance.

RESULTS

KDR Promotes Shade Avoidance Response

We confirmed the upregulation of *KDR* in seedlings of Arabidopsis exposed to a low R:FR treatment (R:FR = 0.2) in comparison to control conditions (R:FR = 2; Fig. 1A). To further investigate the role of KDR in SAS, we studied the response of *kdr* lines to low R:FR conditions. We measured the elongation of hypocotyls in seedlings and of petioles in rosette plants upon exposure to low R:FR. Hypocotyl elongation of a *KDR* knockout line *kdr-1* was reduced in low R:FR conditions, whereas the activation-tagged line *kdr-D*, which results in four times the insertion of the *CaMV 35S* enhancer sequence in the promoter region of *KDR*, displayed an exaggerated elongation (Fig. 1B). When the same lines were tested for petiole elongation in rosette plants, a similar suppression of the response was found for *kdr-1*, but less severely. By contrast, the overexpressing line *kdr-D* showed no statistically significant difference compared to Col-0 wild type regarding low R:FR-induced petiole elongation. The petiole elongation responses between wild type and mutants were not dependent on day length (Fig. 1C).

Overexpression of *KDR* Stimulates Shade Avoidance

We created novel lines overexpressing *KDR* in Arabidopsis Col-0 background in order to have improved genetic material over the *kdr-D* activation tagging line that only mildly overexpresses *KDR*. We then used four homozygous independent lines to study their response to low R:FR treatment at the seedling stage. We found that most of the novel *35S:KDR* transgenic lines showed an even more exaggerated response than that found for *kdr-D* and additionally displayed constitutive hypocotyl elongation in white light (Fig. 2A). Interestingly, the variation in hypocotyl length between the independent transgenic lines correlated with variation in *KDR* overexpression levels (Fig. 2, B and C). We selected the two independent lines with the highest *KDR* expression levels for further analyses. When looking more carefully at the phenotype of the selected lines, we observed that *KDR* overexpression increased elongation of most organs, including hypocotyl, petioles of cotyledons, petioles of true leaves, and primary root (Fig. 2D).

We also verified if petiole elongation in adult plants was affected in our strong overexpression lines. Interestingly, they did not show an increased petiole

Downloaded on January 21, 2021. - Published by https://plantphysiol.org
Copyright (c) 2020 American Society of Plant Biologists. All rights reserved.

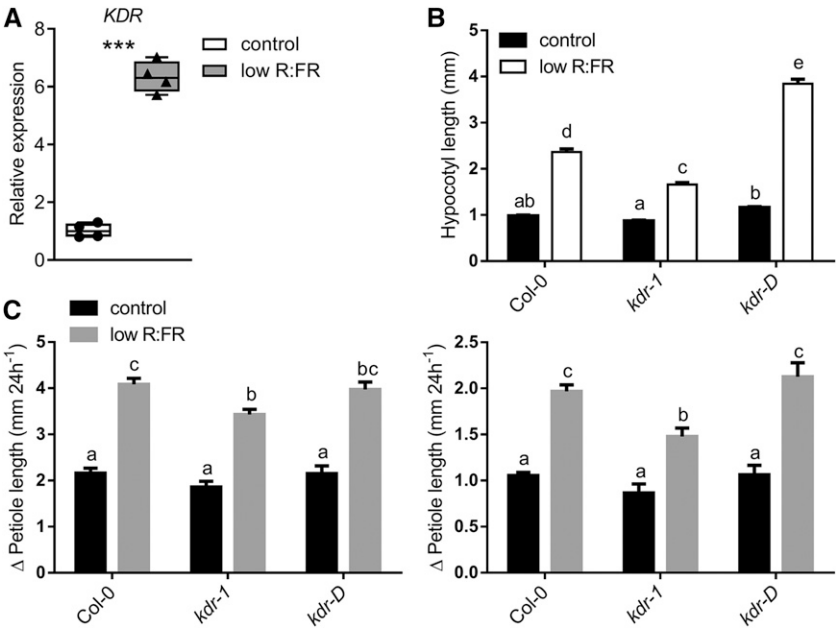

Figure 1. Arabidopsis *kdr* mutants exhibit a deviating low R:FR response. A, Relative expression of *KDR* determined by RT-qPCR in wild-type Col-0 shoots grown in control light conditions (R:FR = 2) and low R:FR (R:FR = 0.2) for 90 min. Data represent means ± SE, $n = 4$. Asterisks indicate statistically significant difference by Student's *t* test (***$P < 0.001$). B, Hypocotyl length of seedlings of Arabidopsis wild type (Col-0), knockout line (*kdr-1*), or activation-tagged line (*kdr-D*) grown in control light conditions (R:FR = 2) or low R:FR (R:FR = 0.2) after 5 d of light treatment. Data represent means ± SE, $n = 76$. C, Change in petiole length (Δ Petiole length) of Arabidopsis wild-type (Col-0) rosette plants, knockout line (*kdr-1*), or activation-tagged line (*kdr-D*) grown in control light conditions (R:FR = 2) or low R:FR (R:FR = 0.2) after 24 h of light treatment. Plants were grown in short (left)- or long-day (right) conditions. Data represent means ± SE, $n = 10$. Different letters indicate statistically significant differences by two-way ANOVA with post-hoc Tukey test ($P < 0.05$).

elongation response to low R:FR treatment (Supplemental Fig. S1A). The *KDR* overexpression lines in adult stage are relatively small, but they do have relatively elongated petioles with small leaf laminas (Supplemental Fig. S1B), reminiscent of a shade avoidance phenotype. The shade avoidance characteristics are highly consistent with increased *KDR* expression. The severe overall growth inhibition, however, might be associated with ectopic expression of *KDR*, possibly in tissue types or developmental stages where it would not normally be expressed. Interestingly, another leaf response, upward movement called hyponasty, was mildly affected in *KDR* overexpression lines (Supplemental Fig. S1C). The hyponastic responses of the overexpression lines seemed to be enhanced, especially at an early time point. Finally, *KDR* overexpression lines also exhibit constitutive early bolting and flowering (Fig. 3; Supplemental Fig. S2A), which is another established shade avoidance response (Halliday et al., 1994). It is also possible that the very high *KDR* expression in these lines accelerates the transition to reproduction early so that fewer resources are invested in vegetative growth. The *KDR* overexpressors had very long flowering stems, which at a later life stage started to split open leading to a more bent flowering architecture, possibly another side effect of the ectopic expression of *KDR* (Supplemental Fig. S2B).

Overexpression of *KDR* Affects Regulation of PIF Targets

The main function of KDR described in the literature is its interaction with the negative growth regulator HFR1, which binds to PIFs and therefore interferes with the transcriptional activation of their target genes responsible for the induction of shade avoidance responses. We therefore verified if some of the well-known PIF targets were transcriptionally regulated in seedling of Arabidopsis overexpressing *KDR* in control white light conditions in comparison to Col-0. Interestingly, some of the PIF targets were significantly upregulated in the two independent overexpression lines, such as *HFR1*, *PHYTOCHROME INTERACTING FACTOR 3-LIKE1* (*PIL1*), and *XYLOGLUCAN ENDOTRANSGLUCOSYLASE/HYDROLASE 17* (*XTH17*), whereas several other targets, especially the auxin-related genes *YUCCA8* (*YUC8*), *INDOLE-3-ACETIC ACID INDUCIBLE29* (*IAA29*), and *IAA19*, were downregulated in the *KDR* overexpression lines compared to Col-0 (Supplemental Fig. S3). It was recently confirmed that KDR could be involved in auxin responses but in a rather contradictory way. Zheng et al. (2017) showed that in protoplasts of cells overexpressing *KDR*, the expression of the auxin response reporter *DR5::GUS* was reduced, whereas it was increased in protoplasts derived from the *KDR* knockout line. Since KDR was identified as an atypical TF, the repression of auxin response caused by *KDR* overexpression does not likely result from direct regulation of the expression of auxin responsive genes, but more likely from KDR interference with true TFs involved in a highly complex network of interactions around auxin response. This could be a partially PIF-independent network, since PIF activity would be increased, rather than inhibited, by KDR, and increased PIF activity would promote rather than suppress *DR5::GUS* expression (Sun et al., 2012).

Interactors of KDR from Y2H Screens

We performed a Y2H screen where the coding sequence (CDS) of *KDR* was cloned in frame with the GAL4 DNA-binding domain of the bait vector and used to screen a prey cDNA library of Arabidopsis cloned

Downloaded on January 21, 2021. - Published by https://plantphysiol.org
Copyright (c) 2020 American Society of Plant Biologists. All rights reserved.

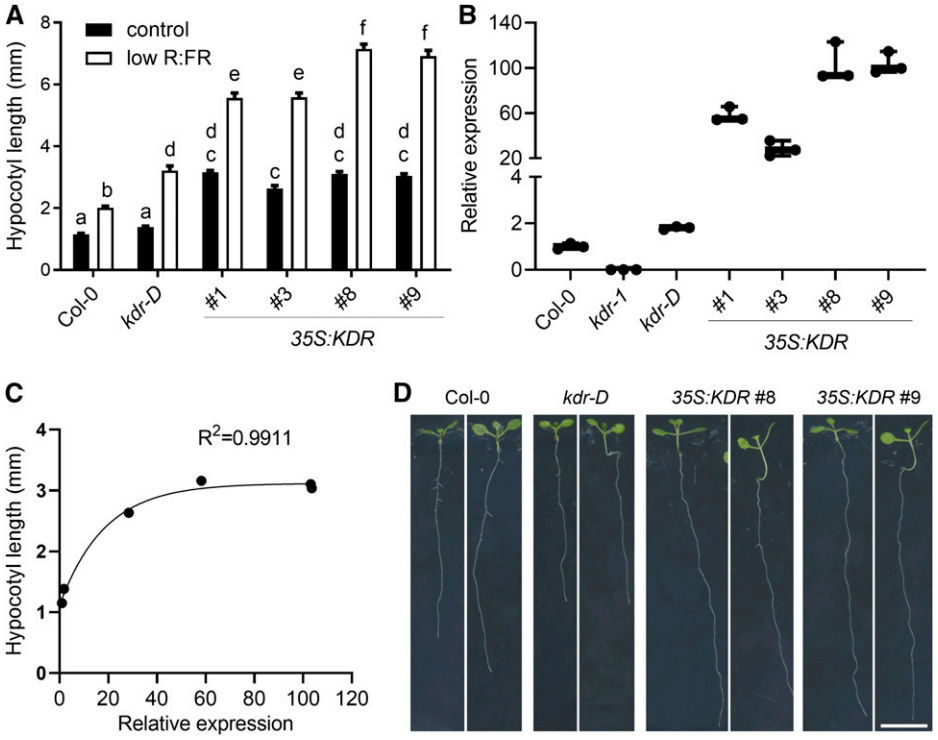

Figure 2. Heterologous overexpression of *KDR* leads to long hypocotyl. A, Hypocotyl length of seedlings of Arabidopsis wild type (Col-0), activation-tagged line (*kdr-D*), and independent homozygous transgenic lines overexpressing *KDR* in Col-0 background grown in control light conditions (R:FR = 2) or low R:FR (R:FR = 0.2) after 5 d of light treatment. Data represent means ± SE, n = 38. Different letters indicate statistically significant differences by two-way ANOVA with post-hoc Tukey test ($P < 0.05$). B, Relative expression level of *KDR* determined by RT-qPCR in wild-type Col-0, knockout line (*kdr-1*), activation-tagged line (*kdr-D*), and independent homozygous transgenic lines overexpressing *KDR* in Col-0 background grown in white light. Data represent means ± SE, $n = 3$. C, Positive correlation between hypocotyl elongation and expression level of *KDR* measured in Col-0, *kdr-D* and in the transgenic lines overexpressing *KDR* using seedlings grown in control light conditions. The correlation was determined by one-phase association curve fitting, equation: $y = y0 + (\text{plateau} - y0)(1 - e^{-kx})$. Parameters, y0 = 1.115; plateau = 3.117; k = 0.05431. D, Representative seedlings of hypocotyl length experiment in A, for each genotype the growth is shown in control light (left) and low R:FR (right). Bar = 1 cm.

with the GAL4 activation domain. The identity of the found interactors are displayed in Table 1, including the frequency with which the interactors were found and the strength of their interaction. Among the proteins identified, we focused on PAR1 and PAR2, two known PIF-interacting proteins. We confirmed the interactions by cloning the full-length CDSs of these proteins (rather than the truncated versions from the library) from Arabidopsis cDNA into the prey vector and using this to retransform yeast to perform a protein-protein interaction assay. In this direct Y2H assay, we also tested the previously published interaction of KDR with HFR1 (Hyun and Lee, 2006; Hong et al., 2013) but could not confirm this interaction (Fig. 4). Also, when swapping the bait-prey configuration, no interaction was found between HFR1 and KDR (Supplemental Fig. S4A). Finally, changing vectors to those used in Hyun and Lee (2006) and Hong et al. (2013; pGBKT7 for the bait and pGADT7 for the prey) again did not confirm the interaction (Supplemental Fig. S4B). To rule out a putatively poor expression of HFR1 in yeast, we verified AD-HFR1 expression in an immunoblot experiment, and this was found to be comparable to AD-PAR1 (Supplemental Fig. S4C). Consistent with proper expression, we also found clear HFR1 homodimerization (Supplemental Fig. S4A), as previously published in Fairchild et al. (2000). As another positive control for the Y2H assays on HFR1, we did confirm interactions of HFR1 with PIF4 and PIF5 (previously published in Hornitschek et al., 2009) and found that HFR1 can also interact with PIF7 (Fig. 5A). We also found that KDR does not directly interact with PIFs in yeast, whereas HFR1 and PAR1 do (Fig. 5A). Lastly, we confirmed that PIF7 can interact with itself and other PIFs (Fig. 5B), which is consistent with the notion that PIFs form hetero- and homodimers to bind DNA regions and activate the expression of target genes (Leivar et al., 2008; Bu et al., 2011).

In order to maximize the number of relevant KDR interactors found, we performed a second Y2H screen using a completely different library consisting of only TFs of Arabidopsis cloned in full-length sequence (Pruneda-Paz et al., 2014). Ten putative interactors were discovered and their identity was verified by sequencing (Table 2). We narrowed the selection for

Downloaded on January 21, 2021. - Published by https://plantphysiol.org
Copyright (c) 2020 American Society of Plant Biologists. All rights reserved.

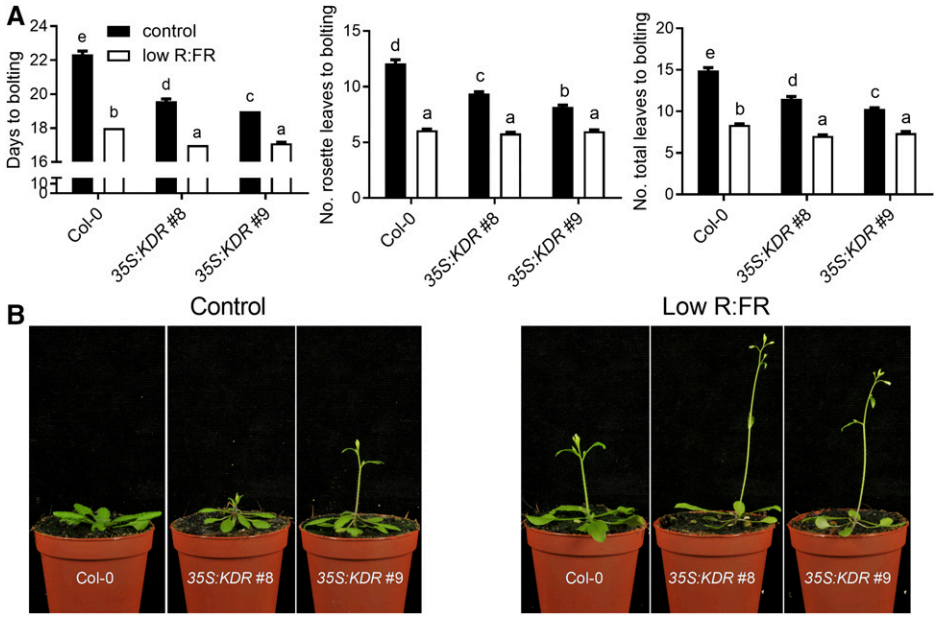

Figure 3. Overexpression of *KDR* leads to a constitutive early flowering. A, Number of days to bolting (left), number of rosette leaves to bolting (middle), and total number of leaves to bolting (right) of Arabidopsis wild type (Col-0) and two independent transgenic lines overexpressing *KDR* in Col-0 background grown in control light conditions (R:FR = 2) or low R:FR (R:FR = 0.2). Data represent means ± SE, $n = 21$. Different letters indicate statistically significant differences by two-way ANOVA with post-hoc Tukey test ($P < 0.05$). B, Representative rosette plants of experiment in A grown for 20 d in pots containing soil.

further studies to four (b)HLH candidates, ACTIVATION-TAGGED BRI1 SUPPRESSOR1 (ATBS1)-INTERACTING FACTOR 2 (AIF2), AIF4, ILI1 BINDING BHLH 1 (IBH1), and IBH1-LIKE 1 (IBL1), since these proteins had previously been linked to growth regulation in association with some regulators of the SAS but had not been implemented in shade avoidance control before. The strength of interaction was verified by performing a Y2H direct interaction assay. All four candidates were able to grow at least up to the medium lacking His and supplemented with 5 mM 3-amino-1, 2, 4-triazole (3-AT), meaning that the interactions were rather strong in yeast (Fig. 4).

KDR Is Localized Mainly in the Nucleus when Coexpressed with Strong Interactors

Next, we investigated the subcellular localization of KDR and its interactors identified with the Y2H screen. KDR was fused in frame to the N-terminal part of a cyan fluorescent protein (CFP), whereas the interactors were fused to the yellow fluorescent protein (YFP). Transient expression in *Nicotiana benthamiana* leaves was carried out and revealed that KDR was localized in both the cytoplasm and the nucleus, as previously published by Hong et al. (2013; Fig. 5C). However, the localization of the interactors appeared exclusively in subcellular compartments of the nucleus. Specifically, HFR1, PAR1, and PAR2 were detected in the nucleoplasm, whereas AIF2, AIF4, IBH1, and IBL1 appeared to be localized in the nucleus but with a very pronounced signal in the nucleolus (Fig. 5C). When KDR was transiently coexpressed with the putative strong interactors, KDR localized exclusively to the nucleus (Fig. 6), indicating that the interaction draws KDR to the nucleus. When coexpressing KDR with HFR1, there was still substantial KDR abundance in the cytoplasm (Supplemental Fig. S4, D and E), similar to when KDR was transiently expressed alone or coexpressed with free YFP, consistent with the lack of interaction described above.

In Planta BiFC Experiments Confirm Interactions in Nuclear Compartments

To further verify the interactions of KDR identified with the Y2H assays, we examined whether they were

Table 1. *List of candidate interactors identified through a Y2H screening of an Arabidopsis cDNA library against KDR*

The strength of interaction is defined as weak when the yeast grew only on SC −Leu −Trp −His medium, as mild when growing up to SC −Leu −Trp −His + 2 mM 3-AT, as medium when yeast grew with the 3-AT increased to 5 mM and as strong when able to grow on SC −Leu −Trp −Ade.

AT Code	Gene Name	Frequency	Strength of Interaction			
			Weak	Mild	Medium	Strong
AT3G58850	*PAR2*	40	1	–	1	38
AT2G42870	*PAR1*	13	–	1	–	12
AT3G11100	*VFP3*	19	–	19	–	–
AT2G32900	*MIP1*	4	–	2	2	–
AT5G57760	–	2	–	–	–	2
AT1G16010	*MRS2-1*	1	–	1	–	–

Downloaded on January 21, 2021. - Published by https://plantphysiol.org
Copyright (c) 2020 American Society of Plant Biologists. All rights reserved.

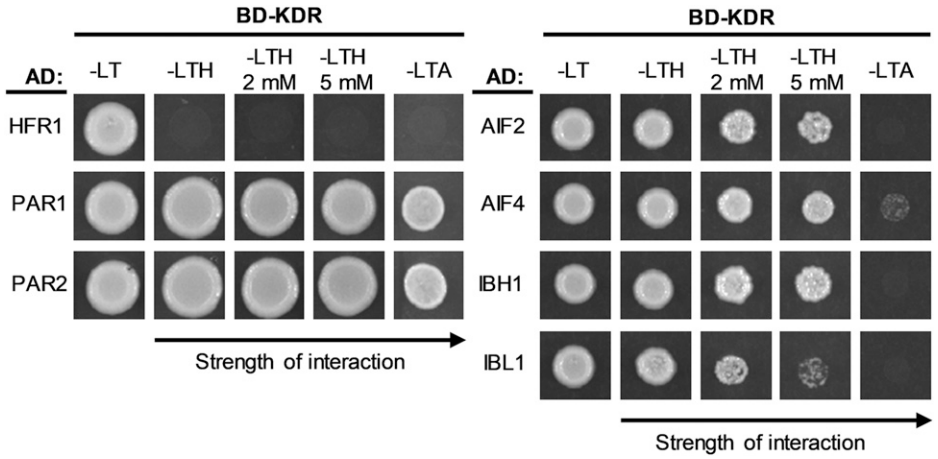

Figure 4. Y2H protein–protein interaction assays confirm the interactions found with screening of two prey libraries of Arabidopsis against the bait KDR. In the GAL4 Y2H assay, the GAL4-DNA binding domain (BD) fused to KDR was coexpressed with the GAL4-activation domain (AD) fused to the full-length CDSs of *HFR1*, *PAR1*, *PAR2* (left) and *AIF2*, *AIF4*, *IBH1*, *IBL1* (right). Yeast cells coexpressing the indicated combinations of constructs were grown on nonselective (−LT) or selective (−LTH + 2 or 5 mM 3-AT and −LTA) media. The strength of interaction is shown by the capability of the yeast to grow on stronger selection media, as indicated by the arrow. L, Leu; T, Trp; H, His; A, adenine.

also occurring in planta. We performed a BiFC assay where the two parts of the split Venus fluorescent protein (YN or YC) were C or N terminally tagged to the proteins of interest and coexpressed in *N. benthamiana* leaves (Fig. 7). We detected the reconstituted YFP signal in the nucleus in all the different samples, apart from the interaction with HFR1, and some differences were noticed when KDR was found to interact with the different candidates. The reconstituted YFP signal was observed in different nuclear compartments, resembling the localization of the targets alone (Fig. 7). The interactions between KDR and PAR1 and PAR2 were observed in the nucleoplasm, whereas the interactions with AIF2, AIF4, IBH1, and IBL1 were found in the nucleus with the strongest signal in the nucleolus. Together, the Y2H and the BiFC data indicate that KDR can truly interact with all the identified targets and that these interactions seem to trigger its translocation primarily to subnuclear complexes, whereas no interaction with HFR1 could be confirmed. No signal was detected when a mutated version of PAR1, namely $PAR1_{L66E}$, in which Leu-66 is mutated to Glu disabling protein-protein interaction (Galstyan et al., 2011), was used in combination with the proteins of interest.

Functional Involvement of KDR Interactors in Shade Avoidance

HFR1, PAR1, and PAR2 were already associated with shade responses and identified as negative regulators of SAS. Somewhat analogous to KDR, they are transcriptional cofactors, which means they regulate transcription without physically binding DNA but by interacting with other proteins through the HLH domain (Roig-Villanova et al., 2007; Galstyan et al., 2011, 2012; Hornitschek et al., 2012). Also, AIF2, AIF4, IBH1, and IBL1 were described as non-DNA-binding (b)HLH proteins (Wang et al., 2009; Ikeda et al., 2012; Zhiponova et al., 2014); however, whereas their role is mainly related to elongation growth, nothing is known so far about shade avoidance in mutants for these genes. We first confirmed that in our conditions *HFR1*, *PAR1*, and *PAR2* were also upregulated following a low R:FR treatment in seedlings of Col-0 (Fig. 8A). Since *AIF2*, *AIF4*, *IBH1*, and *IBL1* were never associated with shade responses, we also verified if their expression level was differentially regulated upon exposure to low R:FR and we found that this was indeed the case (Fig. 8A).

Next, we studied the response to low R:FR conditions of different mutant and overexpression lines of these bHLH genes relative to Col-0 wild type (Fig. 8, B–D). Figure 8, B and C, show that low R:FR-induced hypocotyl elongation is increased in the *hfr1-201*, *hfr1-5*, and *PAR RNAi* line *9* mutants. Overexpressing any of these genes was sufficient to severely block the response to low R:FR. These phenotypes are entirely consistent with the roles of these proteins as negative SAS regulators. Instead, for the lesser-known genes *AIF2*, *AIF4*, *IBH1*, and *IBL1*, we studied the available T-DNA insertion lines, but unfortunately in the SALK lines for *IBH1*, we could not detect the T-DNA insertion and were therefore discarded. In low R:FR conditions, all the lines except for *aif2-2* showed a moderately enhanced hypocotyl elongation response compared to Col-0 wild type (Fig. 8D). In the case of *ibl1*, a statistically significant difference, although minimal, was already seen in control conditions when compared to the wild type. The relatively mild phenotypes, albeit reproducible and statistically significant, may hint at genetic redundancy between the different KDR targets.

Downloaded on January 21, 2021. - Published by https://plantphysiol.org
Copyright (c) 2020 American Society of Plant Biologists. All rights reserved.

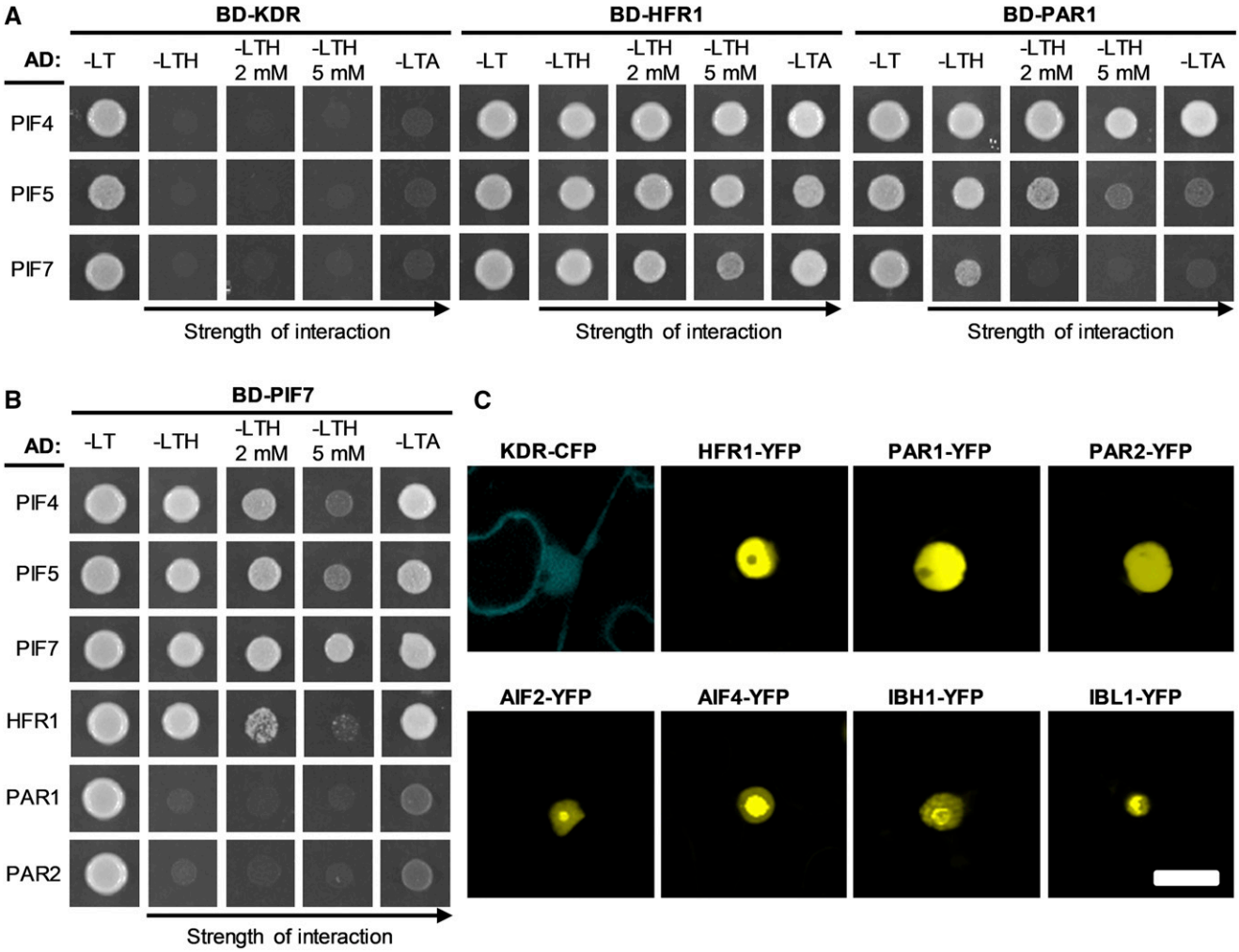

Figure 5. Y2H protein–protein interaction studies and subcellular localization of KDR and its targets in planta. A, In the GAL4 Y2H assay, the GAL4 DNA-binding domain (BD) fused to KDR (left), HFR1 (middle), and PAR1 (right) was coexpressed with the GAL4-activation domain (AD) fused to PIF4, PIF5, and PIF7. The mating of the yeast was confirmed through the growth on nonselective medium (−LT). The assay showed that whereas the bait KDR does not interact with the preys PIF4, PIF5, and PIF7, the bait HFR1 does interact with PIF4, PIF5, and PIF7. PAR1 interacts most strongly with PIF4 and PIF5. B, PIF7 can interact with other PIFs in yeast. When used as bait, PIF7 interacts with the prey HFR1 but not with PAR1 and PAR2. C, KDR fused to CFP and the interactors HFR1, PAR1, PAR2, AIF2, AIF4, IBH1, and IBL1 fused to YFP were transiently expressed in epidermal leaf cells of *N. benthamiana* using *A. tumefaciens*. Images were taken 2 d after agroinfiltration. Scale bar = 20 μm. L, Leu; T, Trp; H, His; A, adenine.

Higher order combinations of these mutants, as well as overexpression lines for these genes, would likely help understand the impact of these shade avoidance components in more detail.

Genetic Interaction between KDR and Downstream Shade Avoidance Regulators

We hypothesized that KDR would act to sequester negative regulators, such as PAR2, by direct interaction. We verified this hypothesis by crossing a *PAR2* overexpression line with a *KDR* overexpression line. The high KDR abundance was expected to sequester PAR2 and restore elongation growth in the *PAR2* overexpressor (Fig. 9). Indeed, we showed that *KDR* overexpression fully rescues hypocotyl elongation and response to low R:FR in the *PAR2* overexpression line. Interestingly, *KDR* overexpression could not rescue low R:FR-induced hypocotyl elongation in an *HFR1* overexpression line, but it could induce elongation in control conditions, similar to observations by Hong et al. (2013), where a combined *KDR* × *HFR1* double overexpression line was exposed to monochromatic B light. Since *PAR2* and *HFR1* overexpression alone did not significantly affect hypocotyl lengths in control light, and the *KDR* × *PAR2* and *KDR* × *HFR1* overexpression lines were as elongated in control light as the *KDR*

Downloaded on January 21, 2021. - Published by https://plantphysiol.org
Copyright (c) 2020 American Society of Plant Biologists. All rights reserved.

Table 2. *List of candidate interactors identified with a screen of a TF library of Arabidopsis against KDR*

AT Code	Type	Gene Name	Involved In
AT4G02590	bHLH	*UNE12*	Fertilization
AT2G31210	bHLH	*bHLH091*	Developing Arabidopsis anther
AT2G28160	bHLH	*FIT*	Regulation of iron uptake responses
AT1G64625	bHLH	*LHL3*	Controlling male meiotic entry
AT2G31280	bHLH155-like protein	*LHL2*	Regulation of early xylem development downstream of auxin
AT3G11100	trihelix	*VFP3*	Interaction with agrobacterium virulence protein VirF
AT3G06590	bHLH	*AIF2*	Negative regulation of cell elongation
AT1G09250	bHLH	*AIF4*	
AT2G43060	bHLH	*IBH1*	Repressing the expression of PIF4
AT4G30410	bHLH	*IBL1*	

overexpression line alone, we conclude that in control white light, PAR2 and HFR1 do not control hypocotyl length, nor does a putative interaction with KDR. It is possible that in control white light, KDR interactions with other proteins, such as AIF2, AIF4, IBL1, and IBH1 (Figs. 4 and 7) is causal to the elongated phenotype, whereas interaction with PAR2 plays a more prominent role under low R:FR light conditions. The observed phenotypes of the different overexpressor combinations are consistent with the observations that KDR interacts with PAR2, and with our observation that KDR does not seem to show interaction with HFR1 to functionally control plant development in low R:FR light conditions. Comparable results were also found when *PAR2* and *HFR1* overexpressor lines were crossed with the mild overexpression line *kdr-D*. Also, here the *HFR1* overexpressor phenotype could not be rescued, whereas the elongation of the hypocotyl of *PAR2* overexpressor was comparable to that of *kdr-D*. A closer look at this cross shows that the appearance of the cotyledons and their "petioles" are similar to those exhibited by *35S:PAR2* overexpression line (Supplemental Fig. S5).

Finally, we also generated transgenic lines overexpressing *KDR* in *pif7*, *pif4 pif5*, and *pif4 pif5 pif7* backgrounds by floral dipping these mutants with a *35S:KDR* construct using *Agrobacterium*-mediated transformation. We then studied their response when exposed to low R:FR using three independent lines for each background, after we verified their expression level (Fig. 10; Supplemental Fig. S6). As expected, *pif4 pif5* shows a clear but reduced response to low R:FR, whereas *pif7* and *pif4 pif5 pif7* lost the hypocotyl response to low R:FR completely. Interestingly, in control light conditions, the overexpression of *KDR* is able to induce a strong elongation in *pif7* and *pif4 pif5* backgrounds, and more mildly when overexpressed in the triple knockout *pif4 pif5 pif7*. When these lines were exposed to low R:FR, *pif4 pif5 35S:KDR* had nearly the same hypocotyl phenotype as the same construct has in wild-type background, consistent with the relatively modest role of *pif4 pif5* in low R:FR-induced hypocotyl elongation. By contrast, in the *pif4 pif5 pif7* mutant, *KDR* overexpression could not rescue the hypocotyl elongation response to low R:FR, whereas it only slightly rescued the response in *pif7*.

We conclude that KDR interacts with PARs to regulate hypocotyl elongation in response to low R:FR, and this subsequently depends on PIFs, probably because PARs directly interact with PIFs to regulate their activity.

DISCUSSION

Significant discoveries have been made in the past decades to identify the molecular mechanisms through which plants perceive neighbors through light signals and activate the shade avoidance network. A previous transcriptome analysis on two wild *Geranium* species, one shade tolerant and the other shade avoiding, identified *KDR* as a molecular component whose expression was correlated with the ability to display elongation responses to shade (Gommers et al., 2017). Here, we attempted to unravel the role of KDR in SAS and found that overexpression of *KDR* in Arabidopsis resulted in an enhanced response to simulated shade conditions. Therefore, it was proposed that the interaction of KDR with HFR1 would release PIFs so that they could activate shade avoidance. If this would have been the only mode of action of KDR, then lines overexpressing *KDR* should have a similar phenotype to knockout lines of *hfr1*, which is not the case. Moreover, independent studies on nonmodel plants identified *KDR* orthologs as strong candidate regulators of contrasting elongation responses, and in these species no *HFR1* orthologs could be found (van Veen et al., 2013; Gommers et al., 2017). Therefore, we speculated that other interacting partners might exist.

KDR Is a Regulator of Established Shade Avoidance Components

Results from one of the Y2H screens and further in planta confirmations identified PAR1 and its closest homolog PAR2 as interactors of KDR, proteins that were previously associated with SAS (Roig-Villanova et al., 2007; Bou-Torrent et al., 2008; Galstyan et al., 2011, 2012; Hao et al., 2012; Cifuentes-Esquivel et al., 2013; Zhou et al., 2014). However, their interaction with KDR was not previously anticipated, and this sheds

Downloaded on January 21, 2021. - Published by https://plantphysiol.org
Copyright (c) 2020 American Society of Plant Biologists. All rights reserved.

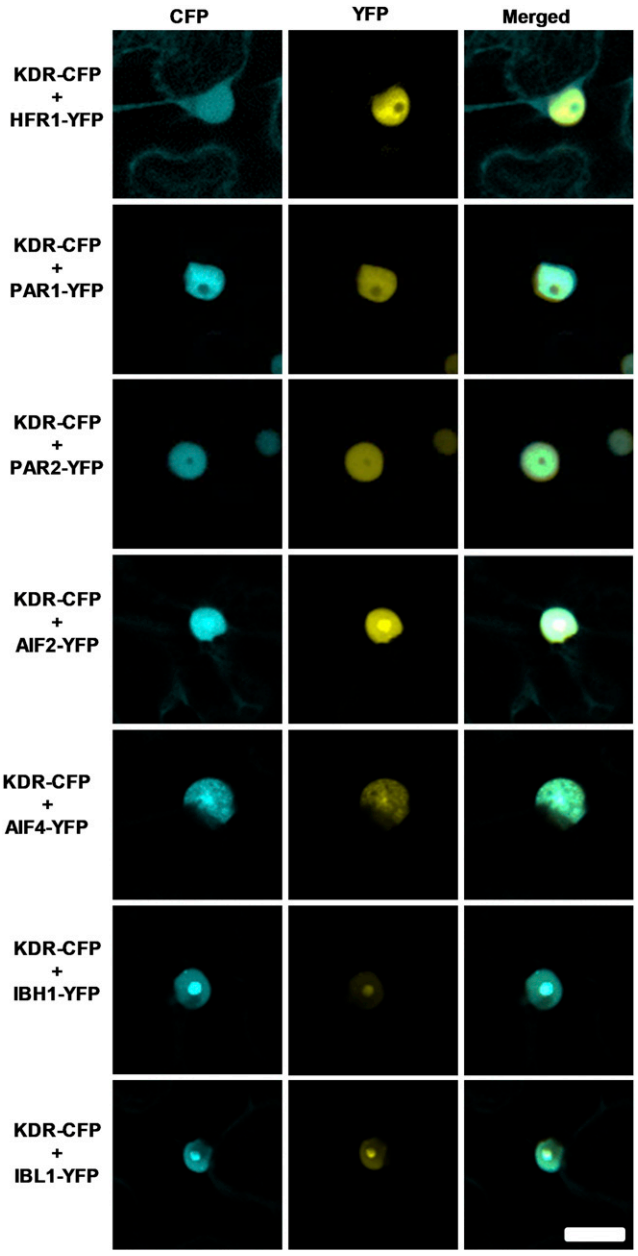

Figure 6. Colocalization of KDR and its interactors in planta. KDR and its interactors were transiently coexpressed in epidermal leaf cells of *N. benthamiana*. KDR was fused to CFP, whereas HFR1, PAR1, PAR2, AIF2, AIF4, IBH1, and IBL1 were fused to YFP. Colocalization observations were made on individual cells, representing individual transformation events (n = 92 [KDR-CFP + HFR1-YFP], 133 [KDR-CFP + PAR1-YFP], 60 [KDR-CFP + PAR2-YFP], 32 [KDR-CFP + AIF4-YFP; KDR-CFP + IBL1-YFP], 36 [KDR-CFP + AIF2-YFP], 39 [KDR-CFP + IBH1-YFP]). Representative images are shown; all cells showed similar localization patterns of the two fluorescently tagged proteins. Images were taken 2 d after infiltration with *A. tumefaciens*. Scale bar = 20 μm.

new light on shade avoidance control. PAR1 and PAR2, as well as KDR and HFR1, are atypical non-DNA-binding (b)HLHs. HFR1 regulates shade avoidance by interacting with several PIFs (PIF1, PIF3, PIF4, and PIF5). This yields nonfunctional complexes unable to bind DNA and therefore blocks the activation of their targets (Hornitschek et al., 2009; Zhang et al., 2013). We show here that HFR1 can also interact with PIF7 (Fig. 5, A and B). Inactivation of PIF4 also occurs via interaction with PAR1 and PAR2, adding an extra level of regulation of cell elongation and plant development. Furthermore, PAR1 can also interact with BES1-INTERACTING-MYC-LIKE1 (BIM1) and with the BRASSINOSTEROID-ENHANCED EXPRESSION1 (BEE1), BEE2, and BEE3, which are positive regulators of SAS, by forming nonfunctional complexes also in this case (Cifuentes-Esquivel et al., 2013). Finally, overexpression of *PRE1*, another (b)HLH member of the same subgroup as KDR, can suppress the dwarf phenotype of *PAR1* overexpression (Hao et al., 2012). In a comparable way, we found that overexpression of *KDR* can restore the growth defect of *PAR2* overexpression (Fig. 9). This finding places KDR in a new third level of SAS regulation, above PAR1 and PAR2, which suppress PIF activity (Fig. 11). Our results cannot confirm the previously described suppressing role of KDR on HFR1, and our genetic data indicate that a putative interaction between HFR1 and KDR is unlikely involved in the regulation of low R:FR-induced hypocotyl elongation.

KDR Interacts with Several Negative Growth Regulators

In this study, we show that KDR physically interacts in yeast and in planta with a range of negative regulators of cell elongation, i.e. AIF2, AIF4, IBH1, and IBL1. None of these proteins have been previously associated with SAS, but they all share some similarities. For example, each of them has been identified already for their interaction with some of the PRE members (Wang et al., 2009; Zhang et al., 2009; Ikeda et al., 2013); they are atypical (b)HLH proteins, unable to bind DNA (Ikeda et al., 2012, 2013); and their overexpression results in a dwarf phenotype (Zhang et al., 2009; Ikeda et al., 2013). Nevertheless, the functions of these proteins remain poorly understood. They have been found to interact with growth-promoting TFs, possibly to suppress the elongation growth (Bai et al., 2012; Ikeda et al., 2012), similar to the mode of action of PARs and HFR1. Furthermore, the dwarf phenotype of *IBH1* overexpression is restored when crossed with an overexpressing line of a *PRE* member (Zhang et al., 2009), reminiscent of the *35S:KDR* #9 × *35S:PAR2* cross shown here (Fig. 9).

In conclusion, KDR interacts with and sequesters (b)HLH transcription cofactors, such as PARs, AIFs, IBH1, and IBL1, which are negative growth regulators. PARs, AIFs, IBH1, and IBL1 bind to the bHLH TFs PIFs, ACTIVATOR FOR CELL ELONGATION1 (ACE1) to ACE3, CRYPTOCHROME-INTERACTING BASIC-HELIX-LOOP-HELIX5 (CIB5), HOMOLOG OF BEE2 INTERACTING WITH IBH1 (HBI1), and BEE2, likely inhibiting their DNA-binding activities to promote cell

Downloaded on January 21, 2021. - Published by https://plantphysiol.org
Copyright (c) 2020 American Society of Plant Biologists. All rights reserved.

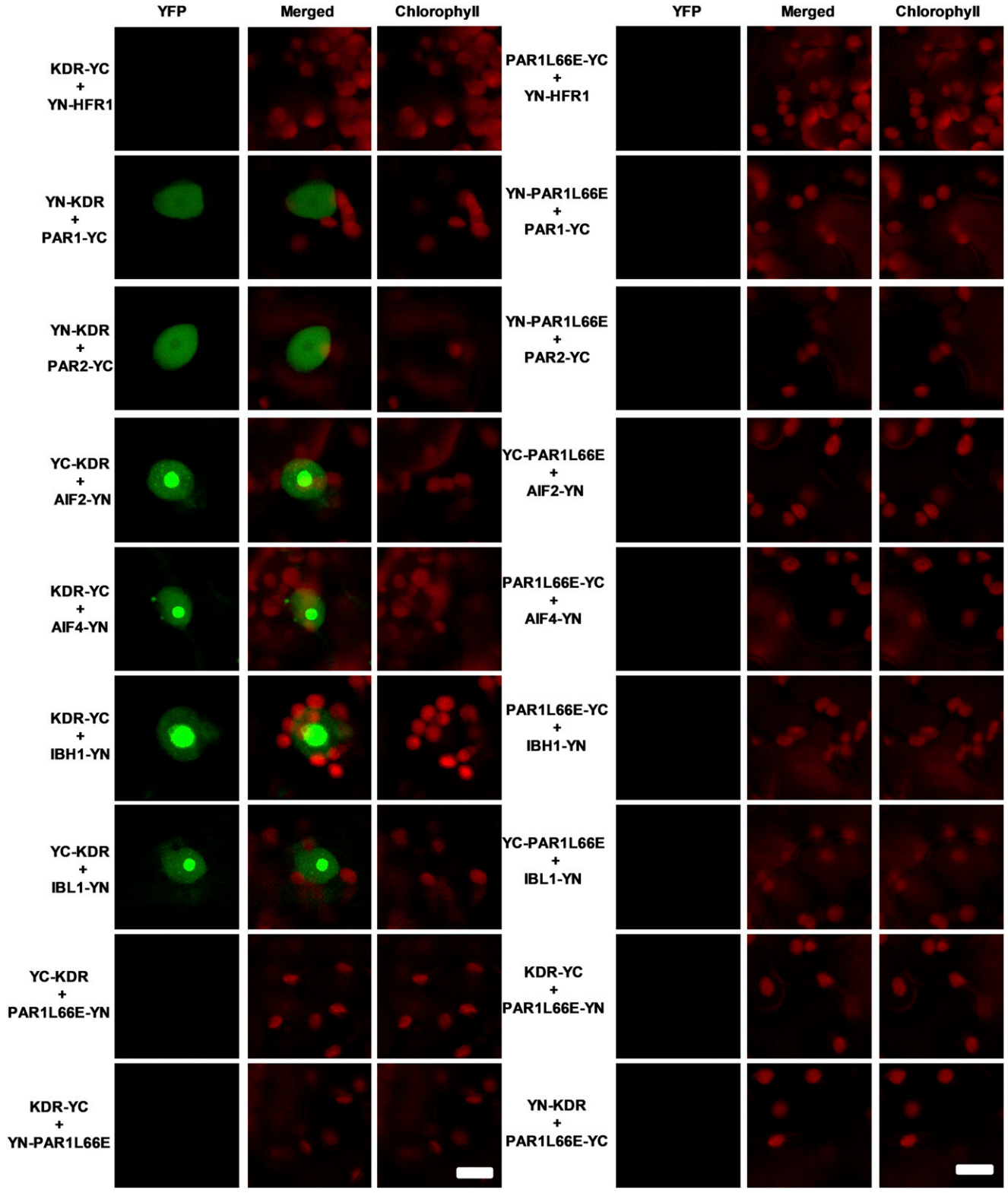

Figure 7. BiFC experiments confirm the interactions found with the Y2H assay. BiFC experiments performed by *A. tumefaciens* transient transformation of *N. benthamiana* leaf epidermis. The interaction of KDR with PAR1, PAR2, AIF2, AIF4, IBH1, and IBL1 was visualized as the reconstituted YFP signal in different nucleus compartments based on the type of interaction. No interaction was found between HFR1 and KDR and the negative controls using PAR1L66E. The autofluorescence of the chloroplasts is shown in red and the BiFC signal of Venus (YFP) in green. Images were taken 2 d after agroinfiltration. Scale bars = 10 μm.

Downloaded on January 21, 2021. - Published by https://plantphysiol.org
Copyright (c) 2020 American Society of Plant Biologists. All rights reserved.

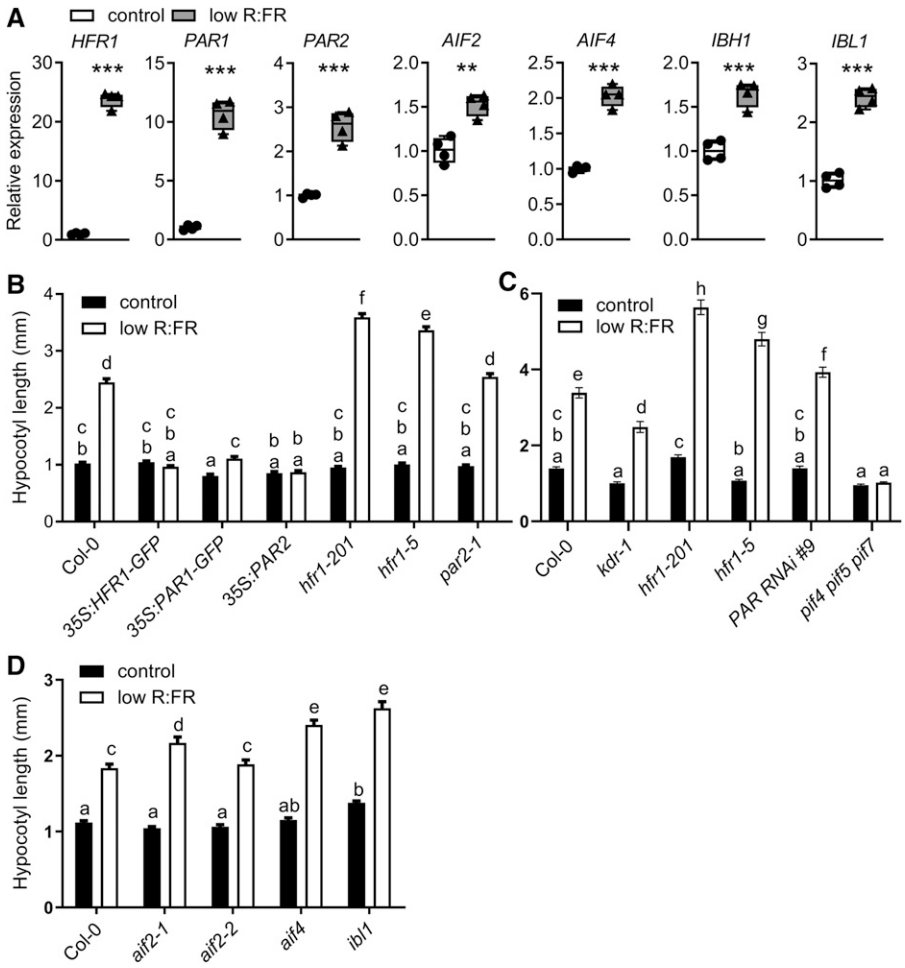

Figure 8. KDR interactors are differentially expressed, and their misexpression affects phenotypic responses to low R:FR. A, Relative expression of *HFR1*, *PAR1*, *PAR2*, *AIF2*, *AIF4*, *IBH1*, and *IBL1* in control white light or low R:FR light for 90 min in wild-type Col-0 shoots. Data represent means ± SE, $n = 4$. Asterisks indicate statistically significant difference by Student's *t* test (***$P < 0.001$ and **$P < 0.01$). B, C, and D, Hypocotyl length of seedlings of Arabidopsis wild type (Col-0), overexpressing lines (*35S:HFR1-GFP*, *35S:PAR1-GFP*, and *35S:PAR2*), and mutants (*hfr1-201*, *hfr1-5*, *PAR RNAi #9*, *pif4 pif5 pif7*, *par2-1*, *aif2-1*, *aif2-2*, *aif4*, and *ibl1*) grown in control light conditions (R:FR = 2) or low R:FR (R:FR = 0.2) after 5 d of light treatment. Data represent means ± SE, $n = 38$. Different letters indicate statistically significant differences by two-way ANOVA with post-hoc Tukey test ($P < 0.05$)

elongation. Upon binding, KDR would then sequester PARs, AIFs, IBH1, and IBL1 so they are kept from binding their bHLH TF targets. This triantagonistic network of bHLHs fine-tunes general plant development as well as adaptation to environmental changes, i.e. changes in light quality. Although under natural conditions, each of these proteins has subtle impacts on development and plasticity, overexpression of these factors leads to a severe dwarfing phenotype and impaired cell elongation, in agreement with their inhibition of positive growth regulators (Zhang et al., 2009; Ikeda et al., 2013; Zhiponova et al., 2014). By contrast, ectopic expression of *KDR* leads to a strongly elongated phenotype. To test if the activity of these negative growth regulators is really inhibited by interaction with KDR, lines overexpressing *KDR* and the negative growth regulators at the same time could test this hypothesis, similar to our data here for combined *PAR2* and *KDR* overexpression (Fig. 9). Alternatively, combinations of loss-of-function alleles for several of the KDR-interacting factors, combined with *kdr* loss of function, could further establish if these interactors act redundantly or if specific functions are associated with specific interaction pairs.

The Heterodimerization of KDR Leads to Its Nuclear Translocation

The interaction of KDR with the (b)HLH cofactors shown here is also reinforced by its translocation from the cytoplasm to the nucleus when coexpressed with the interacting bHLHs identified in the Y2H (Fig. 6). Since bHLH proteins are a family of TFs, they are thought to be localized mostly in the nucleus, where they can regulate the transcription of genes. On the other hand, literature presents evidence showing that the translocation from the cytoplasm to the nucleus is an important posttranslational regulatory mechanism in response to different stimuli and to different plant developmental stages (McGonigle et al., 1996; Nayar et al., 2014; Cui et al., 2016). A possible explanation for KDR translocation is that it could have a weak nuclear localization signal (NLS), whereas its interactors could have a strong NLS and therefore are localized only in the nucleus, even in absence of KDR. Consequently, the predominantly nuclear localization of KDR would rely on partners harboring strong NLS. Indeed, this is another possible mechanism of modulating SAS. In fact, all the strong interactors identified here are upregulated

Downloaded on January 21, 2021. - Published by https://plantphysiol.org
Copyright (c) 2020 American Society of Plant Biologists. All rights reserved.

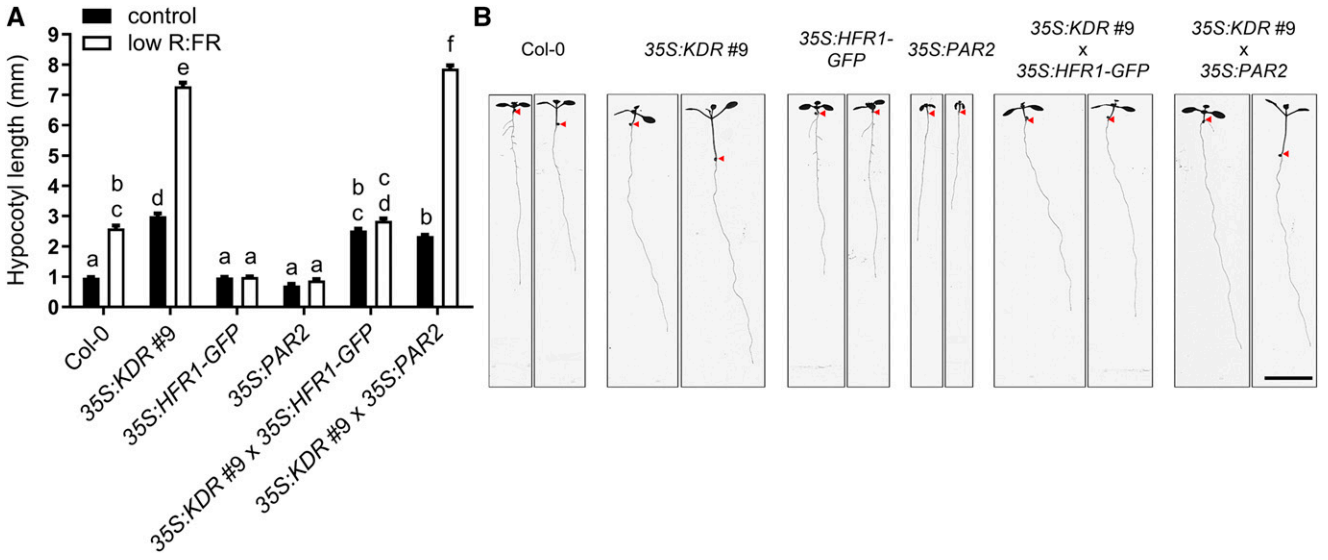

Figure 9. Overexpression of *KDR* rescues hypocotyl length in response to low R:FR in *PAR2* but not *HFR1* overexpressor. A, Hypocotyl length of seedlings of Arabidopsis wild type (Col-0), *35S:KDR* #9; *35S:HFR1-GFP*, and *35S:PAR2* overexpression lines and the double overexpression lines *35S:KDR* #9 × *35S:HFR1-GFP* and *35S:KDR* #9 × *35S:PAR2* grown in control light conditions (R:FR = 2) or low R:FR (R:FR = 0.2) after 5 d of light treatment. Data represent means ± SE, $n = 38$. Different letters indicate statistically significant differences by two-way ANOVA with post-hoc Tukey test ($P < 0.05$) B, Representative seedlings as in experiment (A), for each genotype the growth is shown in control light (left) and low R:FR (right). The arrows indicate the hypocotyl-root transition. Scale bar = 1 cm.

following exposure to low R:FR, suggesting that KDR could change its localization during shade to form heterodimers with the negative growth regulators, inhibiting their function and having as final output the promotion of cell elongation through the release of the other positive growth regulators.

Several Triantagonistic (b)HLH/(b)HLH/bHLH Modules Control Cell Elongation in Response to Multiple Stimuli

Taken together, we propose that the response to shade is mediated by the coaction of several modules of heterodimers formed between bHLH proteins with opposite function in the regulation of elongation

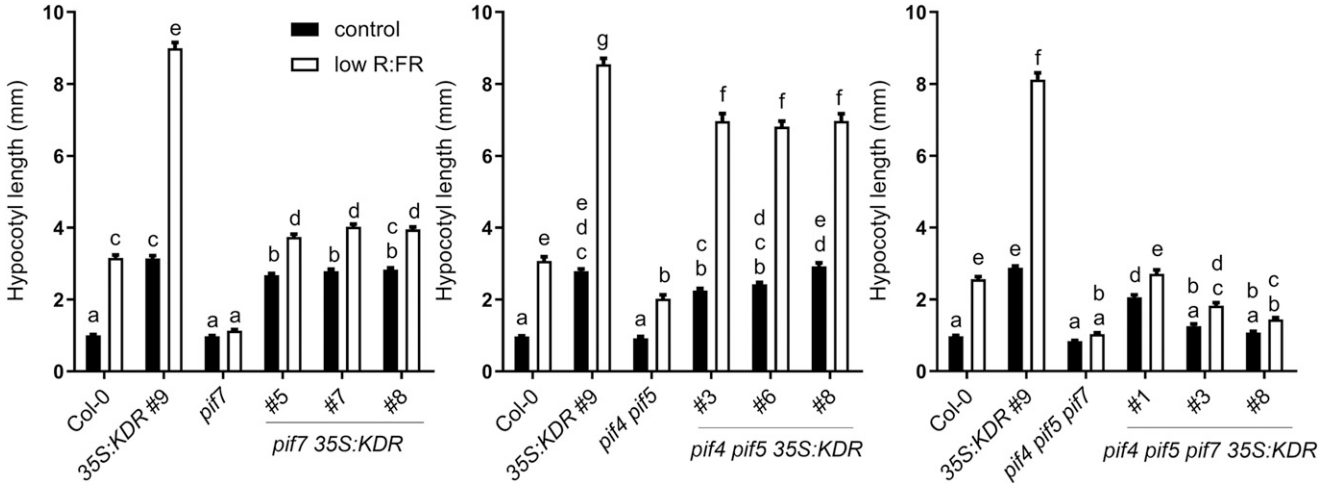

Figure 10. Overexpression of *KDR* in different *pif* knockout lines. Hypocotyl length of seedlings of Arabidopsis wild type (Col-0), knockout lines (*pif7*, *pif4 pif5*, and *pif4 pif5 pif7*), *KDR*-overexpressing line (*35S:KDR* #9), and independent lines of *pif7*, *pif4 pif5*, and *pif4 pif5 pif7*-overexpressing *KDR* (*pif7 35S:KDR*, *pif4 pif5 35S:KDR*, and *pif4 pif5 pif7 35S:KDR*) in control light conditions (R:FR = 2) or low R:FR (R:FR = 0.2) after 5 d of light treatment. Data represent means ± SE, $n = 38$. Different letters indicate statistically significant differences by two-way ANOVA with post-hoc Tukey test ($P < 0.05$).

Downloaded on January 21, 2021. - Published by https://plantphysiol.org
Copyright (c) 2020 American Society of Plant Biologists. All rights reserved.

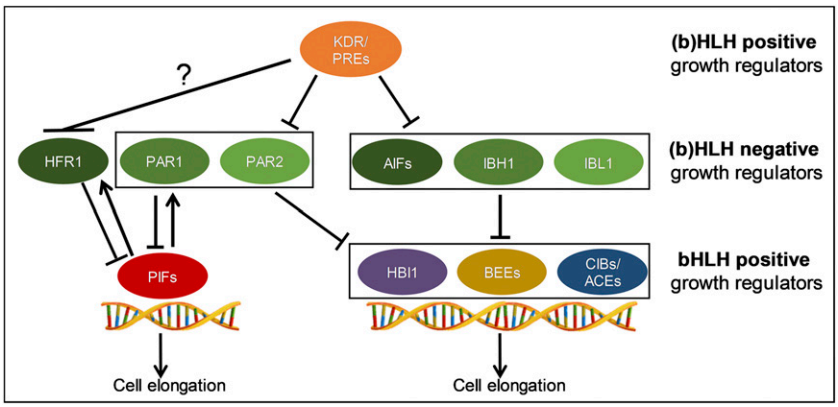

Figure 11. Proposed network regulating cell elongation in low R:FR. The HHbH module is composed of atypical (b)HLH and typical bHLH members, which can be positive or negative growth regulators, and they interact in an antagonistic and redundant manner to regulate cell elongation adequately and rapidly.

(Fig. 11). Furthermore, we conclude that KDR can regulate a substantial number of shade avoidance regulators, certainly many more than previously anticipated, and this would explain the profound impact of variations in *KDR* expression levels on shade avoidance. Some of them are well known negative regulators of shade avoidance responses, i.e. PAR1 and PAR2 (Sessa et al., 2005; Roig-Villanova et al., 2006, 2007), whereas the other interactors found, i.e. AIF2, AIF4, IBH1, and IBL1, had never been associated with shade avoidance. The expression levels of each of these KDR interactors were induced upon low R:FR treatment, consistent with their involvement in the regulation of shade avoidance (Fig. 8A).

The results described here uncovered further levels of shade avoidance regulation and also indicated that HFR1 and KDR might act independently to regulate low R:FR-induced hypocotyl elongation. The gas-and-brake mechanism of different layers of (b)HLH proteins described here gives tremendous opportunity to fine-tune shade avoidance expression. This could be instrumental to enhancing low R:FR response by simultaneous B-light deprivation (de Wit et al., 2016) or suppressing it during abiotic stress (Hayes et al., 2019). Unraveling the exact roles of these bHLH interactions through different life stages of the plant under different light conditions and in other stress response pathways would enable an integrative understanding of plant shade avoidance.

MATERIALS AND METHODS

Plant Material, Growth Conditions, and Measurements

Arabidopsis (*Arabidopsis thaliana*) lines are all in Col-0 background. The following published lines were used: the activation-tagged line *kdr-D* and the knockout *kdr-1* (SALK_048383C; Hyun and Lee, 2006; Gommers et al., 2017), *35S:HFR1-GFP* (also called *G-BH* 03; Galstyan et al., 2011), *35S:PAR1-GFP*, *hfr1-201* (Zhou et al., 2014), *35S:PAR2*, *par2-1*, *PAR RNAi* #9 (Roig-Villanova et al., 2007), *hfr1-5* (Sessa et al., 2005), *pif7-1* (Leivar et al., 2008), *pif4-101 pif5-1* (Lorrain et al., 2008), and *pif4-101 pif5-1 pif7-1* (de Wit et al., 2015). In addition, seeds of *aif2-1* (SALK_ 011076C), *aif2-2* (SALK_ 061834), *aif4* (GK-428G06), and *ibl1* (SALK_119457C; Zhiponova et al., 2014) were obtained from the Nottingham Arabidopsis Stock Centre (NASC, UK) and genotyped using the primers listed in Supplemental Table S1. *35S:HFR1-GFP x kdr-D* and *35:PAR2 x kdr-D* were created by crossing the respective genotypes described above, and experiments were performed using lines homozygous for both inserts.

The plants were cold stratified for 4 d on soil:perlite mix 1:2 (Primasta) supplemented with nutrients (2.6 mM KNO_3, 2 mM $Ca[NO_3]_2$, 0.6 mM KH_2PO_4, 0.9 mM $MgSO_4$, 6.6 μM $MnSO_4$, 2.8 μM $ZnSO_4$, 0.5 μM $CuSO_4$, 66 μM H_3BO_3, 0.8 μM Na_2MoO_4, and 134 mM Fe-EDTA; pH 5.8) and then moved to a growth chamber under short-day conditions (8 h light, 16 h dark; 20°C; 70% humidity; PAR ~140 μmol m^{-2} s^{-1}) for 11 d to allow germination. The plants were then transplanted and left to grow for 3 weeks until the beginning of the experiment. In the case of long-day conditions (16 h light, 8 h dark), the plants were grown for 7 d before being transplanted and then left to grow for an extra week before the light treatment started. Petiole length of the third youngest leaf was measured with a digital caliper before and after the treatment and the difference calculated. Pictures of the same plants were taken before (t = 0) and after the treatment (t = 8 h and t = 24 h), and the Δ in petiole angle was measured with ImageJ (https://imagej.net/Fiji/Downloads) to determine the hyponastic response. For bolting and flowering experiments, a single seed per pot was sown, cold stratified for 4 d, and then moved to the growth chamber under long-day conditions (16 h light, 8 h dark) for 4 d to allow germination before the light treatment started. The number of days to bolting and to flowering was calculated starting from the first day the pots were moved to the growth chamber until the flowering bolt appeared and the first flower opened, respectively. The number of rosette leaves and the total number of leaves (rosette leaves plus cauline leaves) were also measured at the moment of bolting and flowering.

For experiments on Arabidopsis seedlings, the seeds were gas sterilized with chloride for 2 h, sown on sterile square petri dishes (120 × 120 × 17 mm, Greiner Bio One) containing one-half strength Murashige and Skoog (Duchefa Biochemie), 1 g L^{-1} MES hydrate (Sigma-Aldrich), 8 g L^{-1} plant agar (Duchefa Biochemie) at pH 5.8, and cold stratified for 4 d. The plates were placed in the light for 2 h followed by 1 d of darkness and then back to the light for 2 d, after which the light treatment started. The plates were finally scanned, and the hypocotyls were measured with ImageJ.

Nicotiana benthamiana seeds were germinated for 7 d (16 h light, 8 h dark; 20°C; 70% humidity; PAR ~140 μmol m^{-2} s^{-1}) in 9 × 9 × 9.5-cm pots containing soil:perlite mix (1:2; Primasta). The seedlings were then transplanted to 7 × 7 × 8-cm pots and grown for 4 to 5 more weeks before agroinfiltration experiments were started.

Light Treatment

For simulated shade conditions, FR LEDs (730 nm, Philips GreenPower) were used to decrease the R:FR ratio from 2 (control conditions) to 0.2 (shade conditions) without changing the PAR (140 μmol m^{-2} s^{-1}, Philips HPI 400 W). The light treatment lasted 5 d when using Arabidopsis seedlings, and 24 h for adult Arabidopsis plants. The light spectra of the different light conditions are shown in Supplemental Figure S7.

RNA Extraction and RT-qPCR

Whole seedling shoots of 4-d-old seedlings growing on plates (Figs. 1A and 8A; Supplemental Fig. S3) and whole seedling shoot of 8-d-old seedlings (Fig. 2C; Supplemental Fig. S6) were used to extract RNA using the RNeasy

Downloaded on January 21, 2021. - Published by https://plantphysiol.org
Copyright (c) 2020 American Society of Plant Biologists. All rights reserved.

mini kit (Qiagen) followed by DNase I (Qiagen) treatment. cDNA synthesis was performed using SuperScript III RNase H$^-$ reverse transcriptase (Thermo Fisher Scientific) together with random primers (Invitrogen). qPCR reactions were conducted in Viia7 real-time PCR (Thermo Fisher Scientific) using the SYBR green Supermix (Bio-Rad). Two technical replicates of three or four biological samples were used to calculate the average gene expression level normalized to the housekeeping genes *AT4G26410* and *AT5G25760* and relative to the expression level of wild-type Col-0 control condition. The primers used for RT-qPCR are listed in Supplemental Table S2.

Gene Cloning and Plant Transformation

The cDNA used to clone *KDR* CDS of Arabidopsis Col-0 was synthesized from RNA derived from leaf. The CDS was amplified using the Phusion DNA polymerase (Thermo Fisher Scientific) with the *att*B primers listed in Supplemental Table S3 and cloned into the Gateway vector pDONR207 (Thermo Fisher Scientific) using the Gateway BP clonase II enzyme mix (Thermo Fisher Scientific). The reaction was used to transform competent cells of *Escherichia coli* DH5α. Colonies growing on the selective medium containing the antibiotic gentamycin (20 μg mL^{-1}) were checked by colony PCR and the plasmid DNA extracted using the QIAprep spin miniprep kit (Qiagen). A restriction reaction was performed on the extracted plasmid DNA, and the positive samples were sequenced. The entry vector with the right sequence was recombined into the Gateway destination vector pFAST-G02 (Shimada et al., 2010) using the Gateway LR clonase II enzyme mix (Thermo Fisher Scientific). The reaction was then used to transform *E. coli* DH5α competent cells. The colonies growing on the antibiotics streptomycin and spectinomycin (100 μg mL^{-1} each) were checked by colony PCR. The plasmid DNA was extracted and double checked with restriction reaction. Less than 10 ng of construct was used to transform competent cells of *Agrobacterium tumefaciens* AGL-1 that were able to grow on the antibiotic rifampicin (20 μg mL^{-1}). Positive colonies growing on the selective antibiotics were confirmed by colony PCR and then used to transform flowering plants of Arabidopsis Col-0, *pif4*, *pif4 pif5*, and *pif4 pif5 pif7* following the protocol of Zhang et al. (2006). Successfully transformed T1 seeds were selected through the GFP signal in dry seeds. T2 lines were selected for single insertion of the transgene using the selectable marker *bar*, which confers resistance to the herbicide Basta (25 μg mL^{-1}; DL-Phosphinothricin, Duchefa Biochemie). Finally, T_3 seeds were screened for homozygosity using the GFP signal, and the insertion of the transgene was confirmed by PCR reaction performed on genomic DNA (gDNA) extracted from homozygous plants using the primers listed in Supplemental Table S4. Experiments were performed using T_3 or T_4 seeds.

Thermal Asymmetric Interlaced PCR

Leaf material was used to extract gDNA from transgenic lines *35S:KDR* lines 1, 3, 8, and 9, created using the pFAST-G02 vector, as described above. The gDNA was used to perform a thermal asymmetric interlaced PCR (TAIL-PCR) reaction as described in Liu et al. (1995) with minor modifications, using arbitrary degenerate, T-DNA left border end primers (Supplemental Table S5), and DreamTaq DNA polymerase (Thermo Fisher Scientific). The cycle settings used for the TAIL-PCR reactions were adjusted based on the characteristics of the polymerase and primers used and listed in Supplemental Table S6. Purified fragments obtained in the second or third TAIL-PCR reactions were sequenced (Macrogen Europe) and analyzed through a BLAST search (NCBI, www.ncbi.nlm.nih.gov) to identify the flanking sequences. A schematic representation of the insertion sites is shown in Supplemental Figure S8.

Gene Cloning for Y2H Interactions

The procedure for cloning *KDR* CDS was as described before but with the use of the primers listed in Supplemental Table S7 and cloned into the Gateway vector pDONR221 (Thermo Fisher Scientific). The competent cells transformed with the entry vectors were selected for growth on the antibiotic kanamycin (50 μg mL^{-1}). The CDSs of the genes *HFR1*, *PIF4*, *PIF5*, and *PIF7* cloned into the Gateway vector pENTR/D-TOPO and of *PAR1* and *PAR2* cloned into the Gateway vector pENTR223 were obtained from ABRC and sequence validated. The entry vectors containing the CDSs of *KDR*, *HFR1*, *PAR1*, *PAR2*, *PIF4*, *PIF5*, and *PIF7* were recombined into the Gateway destination vector pDEST32 (gentamycin 20 μg mL^{-1}), whereas *KDR*, *HFR1*, *PAR1*, *PAR2*, *PIF4*, *PIF5*, and *PIF7* were also recombined in the Gateway destination vector pDEST22 (carbenicillin 50 μg mL^{-1}). The pDEST22 vectors harboring the CDS of the genes *AIF2*, *AIF4*, *IBH1*, and *IBL1* were obtained from the yeast TF library described by Pruneda-Paz et al. (2014). The yeast colonies were grown on 5-mL liquid synthetic complete (SC) medium (Formedium) lacking the selective amino acid Trp for 1 d at 30°C in shaking conditions. The plasmid DNA was then extracted using the QIAprep spin miniprep kit (Qiagen). Finally, the entry vectors containing *KDR* and *HFR1* were both cloned also into the Gateway destination vectors pGBKT7 (kanamycin 50 μg mL^{-1}) and pGADT7 (carbenicillin 50 μg mL^{-1}).

Yeast Prey Plasmid cDNA Library of Arabidopsis

The yeast prey plasmid cDNA library of Arabidopsis was kindly provided by Dr. Guido van den Ackerveken (Utrecht University, the Netherlands) and created using Invitrogen Custom Services (Invitrogen). RNA was extracted from 15-d-old Arabidopsis seedlings subjected to five conditions: uninfected, infected with a compatible strain of *Hyaloperonospora Arabidopsidis* (*Hpa*), infected with incompatible strain of *Hpa*, sprayed with benzothiadiazole, or infiltrated with NIN-like proteins. This variety of optimal and stress conditions likely yielded a very broad library of different transcripts. Synthesis of cDNA was performed on the RNA extracted, cloned into the Gateway donor vector pENTR222, and then recombined into the Y2H Gateway destination vector pDEST22 to generate a GAL4 activation domain fused to the N-terminal part of Arabidopsis proteins. Competent cells of *Saccharomyces cerevisiae* strain Y8800 (genotype *MATa trp1–901 leu2–3,112 ura3–52 his3–200 Gal4Δ gal80Δ cyh2^R-GAL1:HIS3@LYS2 GAL2:ADE2 GAL7:LacZ@met2*) were transformed with the expression vectors. At least one million colonies were harvested in yeast extract peptone dextrose (YEPD) medium to ensure a good coverage of all the different proteins present in the library. Finally, aliquots of the library were made and stored in glycerol stocks.

Yeast Transformation

The bait constructs cloned into the pDEST32 or pGBKT7 were transformed into the yeast strain Y8930 (genotype *MATα trp1– MATα trp 901 leu2–leu3,112 ura3–ura52 his3–his200 Gal4Δ gal80Δ cyh2^{R}GAL1:HIS3@LYS2 GAL2:ADE2 GAL7:LacZ@met2*), whereas the prey constructs cloned into the pDEST22 or pGADT7 were transformed into the strain Y8800 using the LiAc (Sigma-Aldrich) method (Schiestl and Gietz, 1989). Yeast transformed with the expression vectors pDEST32 and pGADT7 were plated on SC medium lacking the selective amino acid Leu. The same was done for the colonies transformed with the pDEST22 and pGBKT7, but in this case SC was used without the selective amino acid Trp. Four-day-old single colonies growing at 30°C were isolated and the insertion of the plasmids was confirmed with colony PCR using the primers listed in Supplemental Table S8. Positive transformed colonies were resuspended in YEPD containing 24% (v/v) glycerol and stored at −80°C. To test for auto-activation of the bait constructs, yeast strain Y8930 carrying the expression vectors pDEST32 or pGBKT7 were grown on a SC medium lacking His and adenine (Ade) in the following combinations: −Leu −His; −Leu −His + 2 mM 3-AT; −Leu −His + 5 mM 3-AT; and −Leu −Ade for pDEST32 constructs, whereas for colonies carrying the pGBKT7 the medium was lacking Trp instead of Leu. Colonies expressing the proteins PIF4 or PIF5 were able to activate the *HIS3* and *ADE2* reporter genes and for this reason they were not used in the experiments in the bait conformation.

Y2H cDNA Library Screening and Individual Interactions

The Y2H library screening was performed using a mating-based approach described previously (Fromont-Racine et al., 2002). The yeast bait construct expressing *KDR* cloned in the pDEST32 was grown overnight in 10 mL YEPD medium under shaking conditions at room temperature. The day after a 1-mL aliquot of yeast prey cDNA library was thawed on ice, mixed with 100 mL YEPD, and incubated for 1 h. The library was then pelleted at 380*g* for 5 min and washed two times with sterile double distilled water, after which it was resuspended with 10 mL YEPD. Finally, the OD_{600} of the prey library and of the yeast containing the bait construct was measured, and they were mixed in equal amount of $OD_{600} = 6$. The yeast mix was spun down at 380*g* for 5 min, resuspended in 300 μL of sterile double distilled water, and plated on a 10-cm round plate containing YEPD supplemented with carbenicillin (100 μg mL^{-1}). The YEPD plate was incubated at 30°C for 4 h to allow the mating of the yeast. After the incubation, the YEPD plate was washed with 3 mL of sterile double distilled

Downloaded on January 21, 2021. - Published by https://plantphysiol.org
Copyright (c) 2020 American Society of Plant Biologists. All rights reserved.

water, the yeast suspension was collected, centrifuged at 380*g* for 5 min, and the pellet was resuspended in 600 μL of sterile double distilled water. Finally, the yeast was plated on round plates of 15-cm diameter containing SC medium −Leu −Trp −His supplemented with carbenicillin (100 μg mL^{-1}) and incubated at 30°C for 4 d. After the period of incubation, colonies growing on the selective medium were picked, resuspended in 25 μL of sterile double distilled water, and plated on two fresh SC −Leu −Trp −His plates for 2 d at 30°C. Hereafter, individual colonies of yeast from one plate were used for colony PCR using the primers listed in Supplemental Table S8. The resulting product reactions were purified using Agentcourt AMPure XP beads (Beckman Coulter) according to the manufacturer's protocol and sequenced to identify the prey proteins interacting with the bait of interest. The second −Leu −Trp −His plate was replica plated on SC −Leu −Trp −His + 2 mM 3-AT and on SC −Leu −Trp −His + 5 mM 3-AT, which were subsequently incubated for 2 to 3 d at 30°C, and also plated on SC −Leu −Trp −Ade for 5 d at 20°C. Yeast colonies expressing at least one of the two reporter genes were considered positive. A selection of the proteins found in the screening were full-length cloned in the prey vector, as described previously, and the yeast strain Y8800 was transformed. All the baits and the preys used for individual interactions were grown for 2 d at 30°C on SC −Leu or −Trp, based on the type of vectors in which they were expressed. A small dot of a single yeast colony containing the bait or the prey was resuspended in 400 μL of sterile double distilled water. Then 10 μL of prey yeast was mixed with other 10 μL of the bait yeast. Five microliters were spotted on YEPD plate and incubated for 24 h at 30°C to allow the mating and the growth of the yeast. Finally, a small dot of individual mated colony was resuspended in 1 mL of sterile double distilled water and 10 μL was spotted on the following SC selective plates: −Leu −Trp, as confirmation of the mating; −Leu −Trp −His, as confirmation of the interaction; and −Leu −Trp −His + 2 mM 3-AT; −Leu −Trp −His + 5 mM 3-AT; −Leu −Trp −Ade to determine the strength of interaction. The plate lacking Ade was incubated at 20°C for 5 d while all the other plates were incubated at 30°C for 2 to 3 d. The yeast transformed with the empty vector pDEST32 (bait) in combination with the studied preys and the empty vector pDEST22 (prey) in combination with the different baits of interest were used as negative control.

Protein Extraction from Yeast and Detection Using Western Blot

Total protein lysates from yeast harboring the different constructs of pDEST22 were obtained according to the Yeast Protocols Handbook (http://www.takara.co.kr/file/manual/pdf/PT3024-1.pdf; Clontech), following the Urea/SDS method. Before loading, the lysates were boiled for 1 min at 96°C and loaded on a 4% to 15% mini-PROTEAN TGX stain-free protein gels (Bio-Rad). The gels were imaged with a Chemidoc station (Bio-Rad). The separated proteins were subsequently transferred onto a polyvinylidene difluoride membrane using a Bio-Rad transblot turbo. Blots were blocked with 5% (w/v) milk powder (Elk) in Tris-buffered saline (TBS) buffer. Immunodetection of the proteins was performed using the monoclonal antibody directed against the GAL4 activation domain (Clontech no. 630402, 1:1000 in 0.5% [w/v] Elk TBS). Goat anti-mouse IgG conjugated with horseradish peroxidase was used as secondary antibody (Cell Signaling Technology no. 7076, 1:5000 in 0.5% [w/v] Elk TBS plus Tween 20 0.1% [v/v]). The labeled proteins were visualized using 50/50 mix of "pico" and "femto" chemiluminescence substrates (Thermo Fisher) on a ChemiDoc (Bio-Rad).

Yeast Prey Plasmid TF Library of Arabidopsis

The construction of the prey TF library of Arabidopsis was made as described by Pruneda-Paz et al. (2014). In brief, the library consists of 1,956 TFs cloned in full-length sequence (78.5% of all Arabidopsis TFs) into the Gateway pDEST22 vector and expressed in the yeast strain PJ69-4A. The library is divided into 21 96-well plates, and each well contains 100 μL of yeast expressing a single TF mixed to the freezing medium (SC supplemented with 22.5% [v/v] glycerol) and stored at −80°C.

Y2H TF Library Screening

The bait vector pDEST32 harboring the gene *KDR* was used to transform the yeast strain PJ69-4α. The auto-activation of the bait construct was tested by taking a small dot of yeast colony, resuspended in 50 μL of sterile double distilled water, and spotting 5 μL on the selective plates SC −Leu −His containing 0, 5, 10, 15, 20, or 40 mM 3-AT. No auto-activation was found. From the glycerol stock, the bait yeast was grown on SC −Leu at 30°C for 2 d. At the same time, also the yeast of the TFs library was grown, the 96-well plates were thawed on ice, and 5 μL were taken from each single well and spotted on a plate containing SC −Trp and left to grow at 30°C for 2 d. Then, the bait strain was resuspended in 11 mL of sterile double distilled water and 3 μL were spotted on YEPD plates. A small dot of each colony of the library was taken with a pipette tip, resuspended in 200 μL of sterile double distilled water, and 3 μL were spotted on top of the bait. The plates were grown for 3 d at 30°C to allow mating and growth, after which each colony spot was resuspended in 200 μL of sterile double distilled water, and 3 μL was plated on SC −Leu −Trp −His supplemented with 10 mM of 3-AT. The plates were incubated for 3 d at 30°C and then moved to room temperature for 3 extra d. The growth on the yeast was checked after 2, 3, 4, and 6 d to score for interactors. The identity of the positive colonies was confirmed by sequencing the result of a colony PCR used to amplify the Gateway cassette of the pDEST22 carried by the yeast. The primers listed in the Supplemental Table S8 were used to perform the colony PCR.

Gene Cloning for Localization, Colocalization, and BiFC Experiments

For in planta localization and colocalization experiments, cDNA deriving from Arabidopsis was used to amplify the CDSs of *KDR*, *HFR1*, *PAR1*, and *PAR2*, whereas *AIF2*, *AIF4*, *IBH1*, and *IBL1* were amplified from the respective clones in pDEST22 (previously described) using the primers listed in the Supplemental Table S9, which were designed in a way that the CDSs were in frame with a C-terminal tag and without the stop codon. The PCR products containing the *att*B sequences were cloned into the Gateway donor vector pDONR207 (gentamycin 20 μg mL^{-1}). The resulting entry vector containing *KDR* was recombined into the Gateway destination vector pEarleyGate 102 (Earley et al., 2006; kanamycin 50 μg mL^{-1}), whereas *HFR1*, *PAR1*, *PAR2*, *AIF2*, *AIF4*, *IBH1*, and *IBL1* were recombined into the Gateway destination vector pEarleyGate 101 (kanamycin 50 μg mL^{-1}). The empty Gateway destination vector pB7WGY2 was used to visualize the free YFP (Karimi et al., 2005).

For BiFC experiments, the mutated version of PAR1 (called PAR1$_{L66E}$) was amplified from the vector P35S:PAR1$_{L66E}$-G obtained from Galstyan et al. (2011) and cloned into the Gateway donor vector pDONR207. The following set of Gateway destination vectors were used in order to reconstitute the Venus fluorescent protein (YFP): pDEST-^{GW}VYNE (N-terminal part of Venus, residues 1 to 173, referred to as YN in the "Results" section and cloned in frame to the C-terminal part of the protein of interest), pDEST-^{GW}VYCE (C-terminal part of Venus, residues 156 to 239, referred to as YC and cloned in frame to the C-terminal part of the protein of interest), pDEST-VYNE^{GW} (N-terminal part of Venus, residues 1 to 173, referred to as YN and cloned in frame to the N-terminal part of the protein of interest), pDEST-VYCE^{GW} (C-terminal part of Venus, residues 156 to 239, referred as YC in the "Results" section and cloned in frame to the N-terminal part of the protein of interest; Gehl et al., 2009). Transformed competent cells were all selected based on growth on kanamycin (50 μg mL^{-1}). The proteins of this study were cloned without the stop codon when the N- or C-terminal part of the Venus protein was fused to their C-terminal part. They were cloned with the stop codon when the N- or C-terminal part of the Venus protein was fused to their N-terminal part. For each BiFC experiment, we used as positive control the combination of the two interacting proteins published with this BiFC set of vectors (Gehl et al., 2009) and as negative controls the two combinations of empty vectors with the proteins of interest. The combinations of each protein studied here together with the mutated PAR1$_{L66E}$ (Galstyan et al., 2011) were used as additional negative controls.

Transient Expression in *N. benthamiana*

Competent cells of *A. tumefaciens* AGL-1 were transformed with the Gateway expression vectors described in the previous paragraph made for localization, colocalization, or BiFC experiments. Transformed colonies were selected using the antibiotic resistance of the different vectors and with rifampicin (20 μg mL^{-1}) carried by AGL-1 cells. Single colonies were grown for 2 d at 28°C in 20 mL Luria-Bertani medium under shaking conditions. After the OD_{600} was measured, the cells were pelleted and resuspended to a final OD_{600} of 0.5 with a one-half strength Murashige and Skoog medium (Duchefa Biochemie) supplemented with 10 mM MES hydrate (Sigma-Aldrich), 20 g L^{-1} Suc (Sigma-Aldrich), and 200 μM acetosyringone (Sigma-Aldrich) at pH 5.6 and incubated

Downloaded on January 21, 2021. - Published by https://plantphysiol.org
Copyright (c) 2020 American Society of Plant Biologists. All rights reserved.

in darkness for at least 1 h. The solutions were used to agroinfiltrate the abaxial side of 4- to 5-week-old *N. benthamiana* leaves using a 1-mL syringe without the needle. In the case of colocalization or BiFC experiments, the cells of *A. tumefaciens* carrying the two different expression vectors were mixed before performing agroinfiltration. The plants were left to grow in normal light conditions and after 2 d leaf sections were taken from the agroinfiltrated regions and visualized through confocal microscopy.

Confocal Microscopy

Microscopy was performed using a Zeiss LM 700 (Zeiss) confocal laser-scanning microscope using the 20× water immersion objective (Plan-Apochromat 20×/0.8 M27). Fresh leaf material was prepared on a glass slide with a cover slip. Excitation of YFP, CFP, and autofluorescence of chlorophyll was done at 488 nm, 405 nm, and 488 nm, respectively. Light emission of YFP was detected at 493 to 550 nm, CFP at 300 to 483 nm, and chlorophyll autofluorescence at 644 to 800 nm. Pinhole, gain, laser power, and detector offset were always set the same within experiments. Analyses of the images were performed with ZEN lite (blue edition).

Statistical Analysis

Growth data were analyzed by two-way ANOVA followed by post-hoc Tukey test, whereas RT-qPCR data were analyzed by Student's *t* test or one-way ANOVA followed by post-hoc Tukey test. All the analyses were done using GraphPad Prism.

Accession Numbers

Sequence data from this article can be found in the EMBL/GenBank data libraries under the following accession numbers: *AT1G26945* (*KDR*), *AT5G25760*, *AT4G26410*, *AT1G02340* (*HFR1*), *AT2G42870* (*PAR1*), *AT3G58850* (*PAR2*), *AT3G06590* (*AIF2*), *AT1G09250* (*AIF4*), *AT2G43060* (*IBH1*), *AT4G30410* (*IBL1*), *AT2G43010* (*PIF4*), *AT3G59060* (*PIF5*), *AT5G61270* (*PIF7*), *AT2G46970* (*PIL1*), *AT4G14130* (*XTH15*), *AT1G65310* (*XTH17*), *AT5G39860* (*PRE1*), *AT4G28720* (*YUC8*), *AT3G15540* (*IAA19*), and *AT4G32280* (*IAA29*).

Supplemental Data

The following supplemental materials are available.

Supplemental Figure S1. Petiole hyponasty in response to low R:FR in adult *KDR* overexpression lines.

Supplemental Figure S2. *KDR* overexpression lines show altered traits at adult stage.

Supplemental Figure S3. Differential regulation of PIF targets in *KDR* overexpression lines.

Supplemental Figure S4. Y2H protein-protein interaction assays and coexpression studies do not show evidence of interaction between KDR and HFR1.

Supplemental Figure S5. Activation-tagged *kdr-D* rescues the phenotype of *PAR2*, but not *HFR1* overexpression, under low R:FR.

Supplemental Figure S6. Characterization of *KDR* expression level in independent transgenic lines.

Supplemental Figure S7. Spectral composition of the different light conditions used.

Supplemental Figure S8. Schematic representation of T-DNA insertion sites.

Supplemental Table S1. Primers used for genotyping.

Supplemental Table S2. Primers for RT-qPCR.

Supplemental Table S3. Primers with *att*B cloning sites for full-length *KDR* CDS amplification.

Supplemental Table S4. Primers used for genotyping transgenic lines overexpressing *KDR* made using the vector pFAST-G02.

Supplemental Table S5. Primers used for TAIL-PCR.

Supplemental Table S6. Cycle settings used for TAIL-PCR.

Supplemental Table S7. Primers with *att*B cloning sites for full-length *KDR* CDS amplification.

Supplemental Table S8. Primers used for amplification of Arabidopsis gene fragments in Y2H vectors.

Supplemental Table S9. Primers with *att*B cloning sites for CDS amplification without the stop codon.

ACKNOWLEDGMENTS

We would like to thank Guido van den Ackerveken for sharing the Y2H library; Mike Boxem, Manon Neilen and Marciel Pereira Mendes for help with starting Y2H library screenings; Jaime Martínez-García for sharing seeds of several mutants; Yorrit van de Kaa for help with seed propagation and screening of T_2 and T_3 transgenic seeds; Kaisa Kajala for help with setting up the confocal microscope for the localization experiments; and Diederik Keuskamp for help with light spectral calculations.

Received May 27, 2020; accepted September 29, 2020; published October 13, 2020.

LITERATURE CITED

Al-Sady B, Ni W, Kircher S, Schäfer E, Quail PH (2006) Photoactivated phytochrome induces rapid PIF3 phosphorylation prior to proteasome-mediated degradation. Mol Cell **23:** 439–446

Bai M-Y, Fan M, Oh E, Wang Z-Y (2012) A triple helix-loop-helix/basic helix-loop-helix cascade controls cell elongation downstream of multiple hormonal and environmental signaling pathways in Arabidopsis. Plant Cell **24:** 4917–4929

Ballaré CL, Scopel AL, Sánchez RA (1991) Photocontrol of stem elongation in plant neighbourhoods: Effects of photon fluence rate under natural conditions of radiation. Plant Cell Environ **14:** 57–65

Boccalandro HE, Ploschuk EL, Yanovsky MJ, Sánchez RA, Gatz C, Casal JJ (2003) Increased phytochrome B alleviates density effects on tuber yield of field potato crops. Plant Physiol **133:** 1539–1546

Bou-Torrent J, Roig-Villanova I, Galstyan A, Martínez-García JF (2008) PAR1 and PAR2 integrate shade and hormone transcriptional networks. Plant Signal Behav **3:** 453–454

Bu Q, Castillon A, Chen F, Zhu L, Huq E (2011) Dimerization and blue light regulation of PIF1 interacting bHLH proteins in *Arabidopsis*. Plant Mol Biol **77:** 501–511

Chen M, Chory J (2011) Phytochrome signaling mechanisms and the control of plant development. Trends Cell Biol **21:** 664–671

Cifuentes-Esquivel N, Bou-Torrent J, Galstyan A, Gallemí M, Sessa G, Salla Martret M, Roig-Villanova I, Ruberti I, Martínez-García JF (2013) The bHLH proteins BEE and BIM positively modulate the shade avoidance syndrome in *Arabidopsis* seedlings. Plant J **75:** 989–1002

Cui J, You C, Zhu E, Huang Q, Ma H, Chang F (2016) Feedback regulation of DYT1 by interactions with downstream bHLH factors promotes DYT1 nuclear localization and anther development. Plant Cell **28:** 1078–1093

de Wit M, Keuskamp DH, Bongers FJ, Hornitschek P, Gommers CMM, Reinen E, Martínez-Cerón C, Fankhauser C, Pierik R (2016) Integration of phytochrome and cryptochrome signals determines plant growth during competition for light. Curr Biol **26:** 3320–3326

de Wit M, Ljung K, Fankhauser C (2015) Contrasting growth responses in lamina and petiole during neighbor detection depend on differential auxin responsiveness rather than different auxin levels. New Phytol **208:** 198–209

Earley KW, Haag JR, Pontes O, Opper K, Juehne T, Song K, Pikaard CS (2006) Gateway-compatible vectors for plant functional genomics and proteomics. Plant J **45:** 616–629

Fairchild CD, Schumaker MA, Quail PH (2000) HFR1 encodes an atypical bHLH protein that acts in phytochrome A signal transduction. Genes Dev **14:** 2377–2391

Fromont-Racine M, Rain J-C, Legrain P (2002) Building protein-protein networks by two-hybrid mating strategy. **350:** 513–524

Galstyan A, Bou-Torrent J, Roig-Villanova I, Martínez-García JF (2012) A dual mechanism controls nuclear localization in the atypical basic-helix-loop-helix protein PAR1 of *Arabidopsis thaliana*. Mol Plant **5:** 669–677

Downloaded on January 21, 2021. - Published by https://plantphysiol.org
Copyright (c) 2020 American Society of Plant Biologists. All rights reserved.

Galstyan A, Cifuentes-Esquivel N, Bou-Torrent J, Martinez-Garcia JF (2011) The shade avoidance syndrome in *Arabidopsis*: A fundamental role for atypical basic helix-loop-helix proteins as transcriptional cofactors. Plant J **66:** 258–267

Galvão VC, Fiorucci A-S, Trevisan M, Franco-Zorilla JM, Goyal A, Schmid-Siegert E, Solano R, Fankhauser C (2019) PIF transcription factors link a neighbor threat cue to accelerated reproduction in *Arabidopsis*. Nat Commun **10:** 4005

Gehl C, Waadt R, Kudla J, Mendel R-R, Hänsch R (2009) New GATEWAY vectors for high throughput analyses of protein-protein interactions by bimolecular fluorescence complementation. Mol Plant **2:** 1051–1058

Gommers CMM, Keuskamp DH, Buti S, van Veen H, Koevoets IT, Reinen E, Voesenek LACJ, Pierik R (2017) Molecular profiles of contrasting shade response strategies in wild plants: Differential control of immunity and shoot elongation. Plant Cell **29:** 331–344

Gommers CMM, Visser EJW, St Onge KR, Voesenek LACJ, Pierik R (2013) Shade tolerance: When growing tall is not an option. Trends Plant Sci **18:** 65–71

Halliday KJ, Koornneef M, Whitelam GC (1994) Phytochrome B and at least one other phytochrome mediate the accelerated flowering response of *Arabidopsis thaliana* L. to low red/far-red ratio. Plant Physiol **104:** 1311–1315

Hao Y, Oh E, Choi G, Liang Z, Wang ZY (2012) Interactions between HLH and bHLH factors modulate light-regulated plant development. Mol Plant **5:** 688–697

Hayes S, Pantazopoulou CK, van Gelderen K, Reinen E, Tween AL, Sharma A, de Vries M, Prat S, Schuurink RC, Testerink C, et al (2019) Soil salinity limits plant shade avoidance. Curr Biol **29:** 1669–1676.e4

Hong S-YY, Seo PJ, Ryu JY, Cho S-HH, Woo J-CC, Park C-MM (2013) A competitive peptide inhibitor KIDARI negatively regulates HFR1 by forming nonfunctional heterodimers in *Arabidopsis* photomorphogenesis. Mol Cells **35:** 25–31

Hornitschek P, Kohnen MV, Lorrain S, Rougemont J, Ljung K, López-Vidriero I, Franco-Zorrilla JM, Solano R, Trevisan M, Pradervand S, et al (2012) Phytochrome interacting factors 4 and 5 control seedling growth in changing light conditions by directly controlling auxin signaling. Plant J **71:** 699–711

Hornitschek P, Lorrain S, Zoete V, Michielin O, Fankhauser C (2009) Inhibition of the shade avoidance response by formation of non-DNA binding bHLH heterodimers. EMBO J **28:** 3893–3902

Hyun Y, Lee I (2006) KIDARI, encoding a non-DNA binding bHLH protein, represses light signal transduction in *Arabidopsis thaliana*. Plant Mol Biol **61:** 283–296

Ikeda M, Fujiwara S, Mitsuda N, Ohme-Takagi M (2012) A triantagonistic basic helix-loop-helix system regulates cell elongation in Arabidopsis. Plant Cell **24:** 4483–4497

Ikeda M, Mitsuda N, Ohme-Takagi M (2013) ATBS1 INTERACTING FACTORs negatively regulate *Arabidopsis* cell elongation in the triantagonistic bHLH system. Plant Signal Behav **8:** e23448

Karimi M, De Meyer B, Hilson P (2005) Modular cloning in plant cells. Trends Plant Sci **10:** 103–105

Leivar P, Monte E, Al-Sady B, Carle C, Storer A, Alonso JM, Ecker JR, Quail PH (2008) The Arabidopsis phytochrome-interacting factor PIF7, together with PIF3 and PIF4, regulates responses to prolonged red light by modulating phyB levels. Plant Cell **20:** 337–352

Leivar P, Quail PH (2011) PIFs: Pivotal components in a cellular signaling hub. Trends Plant Sci **16:** 19–28

Li L, Ljung K, Breton G, Schmitz RJ, Pruneda-Paz J, Cowing-Zitron C, Cole BJ, Ivans LJ, Pedmale UV, Jung H-S, et al (2012) Linking photoreceptor excitation to changes in plant architecture. Genes Dev **26:** 785–790

Liu YG, Mitsukawa N, Oosumi T, Whittier RF (1995) Efficient isolation and mapping of *Arabidopsis thaliana* T-DNA insert junctions by thermal asymmetric interlaced PCR. Plant J **8:** 457–463

Lorrain S, Allen T, Duek PD, Whitelam GC, Fankhauser C (2008) Phytochrome-mediated inhibition of shade avoidance involves degradation of growth-promoting bHLH transcription factors. Plant J **53:** 312–323

Lorrain S, Fankhauser C (2012) Plant development: Should I stop or should I grow? Curr Biol **22:** R645–R647

McGonigle B, Bouhidel K, Irish VF (1996) Nuclear localization of the *Arabidopsis* APETALA3 and PISTILLATA homeotic gene products depends on their simultaneous expression. Genes Dev **10:** 1812–1821

Molina-Contreras MJ, Paulišić S, Then C, Moreno-Romero J, Pastor-Andreu P, Morelli L, Roig-Villanova I, Jenkins H, Hallab A, Gan X, et al (2019) Photoreceptor activity contributes to contrasting responses to shade in cardamine and Arabidopsis seedlings. Plant Cell **31:** 2649–2663

Nayar S, Kapoor M, Kapoor S (2014) Post-translational regulation of rice MADS29 function: homodimerization or binary interactions with other seed-expressed MADS proteins modulate its translocation into the nucleus. J Exp Bot **65:** 5339–5350

Pantazopoulou CK, Bongers FJ, Küpers JJ, Reinen E, Das D, Evers JB, Anten NPR, Pierik R (2017) Neighbor detection at the leaf tip adaptively regulates upward leaf movement through spatial auxin dynamics. Proc Natl Acad Sci USA **114:** 7450–7455

Pruneda-Paz JL, Breton G, Nagel DH, Kang SE, Bonaldi K, Doherty CJ, Ravelo S, Galli M, Ecker JR, Kay SA (2014) A genome-scale resource for the functional characterization of *Arabidopsis* transcription factors. Cell Rep **8:** 622–632

Robson PRH, McCormac AC, Irvine AS, Smith H (1996) Genetic engineering of harvest index in tobacco through overexpression of a phytochrome gene. Nat Biotechnol **14:** 995–998

Roig-Villanova I, Bou J, Sorin C, Devlin PF, Martínez-García JF (2006) Identification of primary target genes of phytochrome signaling: Early transcriptional control during shade avoidance responses in Arabidopsis. Plant Physiol **141:** 85–96

Roig-Villanova I, Bou-Torrent J, Galstyan A, Carretero-Paulet L, Portolés S, Rodríguez-Concepción M, Martínez-García JF (2007) Interaction of shade avoidance and auxin responses: A role for two novel atypical bHLH proteins. EMBO J **26:** 4756–4767

Schiestl RH, Gietz RD (1989) High efficiency transformation of intact yeast cells using single stranded nucleic acids as a carrier. Curr Genet **16:** 339–346

Sessa G, Carabelli M, Sassi M, Ciolfi A, Possenti M, Mittempergher F, Becker J, Morelli G, Ruberti I (2005) A dynamic balance between gene activation and repression regulates the shade avoidance response in *Arabidopsis*. Genes Dev **19:** 2811–2815

Shen Y, Khanna R, Carle CM, Quail PH (2007) Phytochrome induces rapid PIF5 phosphorylation and degradation in response to red-light activation. Plant Physiol **145:** 1043–1051

Shimada TL, Shimada T, Hara-Nishimura I (2010) A rapid and non-destructive screenable marker, FAST, for identifying transformed seeds of *Arabidopsis thaliana*. Plant J **61:** 519–528

Sun J, Qi L, Li Y, Chu J, Li C (2012) PIF4-mediated activation of YUCCA8 expression integrates temperature into the auxin pathway in regulating *Arabidopsis* hypocotyl growth. PLoS Genet **8:** e1002594

van Veen H, Mustroph A, Barding GA, Vergeer-van Eijk M, Welschen-Evertman RAM, Pedersen O, Visser EJW, Larive CK, Pierik R, Bailey-Serres J, et al (2013) Two Rumex species from contrasting hydrological niches regulate flooding tolerance through distinct mechanisms. Plant Cell **25:** 4691–4707

Wang H, Zhu Y, Fujioka S, Asami T, Li J, Li J (2009) Regulation of Arabidopsis brassinosteroid signaling by atypical basic helix-loop-helix proteins. Plant Cell **21:** 3781–3791

Zhang L-Y, Bai M-Y, Wu J, Zhu J-Y, Wang H, Zhang Z, Wang W, Sun Y, Zhao J, Sun X, et al (2009) Antagonistic HLH/bHLH transcription factors mediate brassinosteroid regulation of cell elongation and plant development in rice and Arabidopsis. Plant Cell **21:** 3767–3780

Zhang X, Henriques R, Lin S-S, Niu Q-W, Chua N-H (2006) Agrobacterium-mediated transformation of *Arabidopsis thaliana* using the floral dip method. Nat Protoc **1:** 641–646

Zhang Y, Mayba O, Pfeiffer A, Shi H, Tepperman JM, Speed TP, Quail PH (2013) A quartet of PIF bHLH factors provides a transcriptionally centered signaling hub that regulates seedling morphogenesis through differential expression-patterning of shared target genes in *Arabidopsis*. PLoS Genet **9:** e1003244

Zheng K, Wang Y, Zhang N, Jia Q, Wang X, Hou C, Chen J-G, Wang S (2017) Involvement of PACLOBUTRAZOL RESISTANCE6/KIDARI, an atypical bHLH transcription factor, in auxin responses in *Arabidopsis*. Front Plant Sci **8:** 1813

Zhiponova MK, Morohashi K, Vanhoutte I, Machemer-Noonan K, Revalska M, Van Montagu M, Grotewold E, Russinova E (2014) Helix-loop-helix/basic helix-loop-helix transcription factor network represses cell elongation in *Arabidopsis* through an apparent incoherent feed-forward loop. Proc Natl Acad Sci USA **111:** 2824–2829

Zhou P, Song M, Yang Q, Su L, Hou P, Guo L, Zheng X, Xi Y, Meng F, Xiao Y, et al (2014) Both PHYTOCHROME RAPIDLY REGULATED1 (PAR1) and PAR2 promote seedling photomorphogenesis in multiple light signaling pathways. Plant Physiol **164:** 841–852

Downloaded on January 21, 2021. - Published by https://plantphysiol.org
Copyright (c) 2020 American Society of Plant Biologists. All rights reserved.